



Creation of the Cocos and Nazca plates by fission of the Farallon plate

Peter Lonsdale*

0205, Scripps Institution of Oceanography, La Jolla, California, 92093, U.S.A.

Received 27 August 2003; accepted 18 May 2005

Available online 27 June 2005

Abstract

Throughout the Early Tertiary the area of the Farallon oceanic plate was episodically diminished by detachment of large and small northern regions, which became independently moving plates and microplates. The nature and history of Farallon plate fragmentation has been inferred mainly from structural patterns on the western, Pacific-plate flank of the East Pacific Rise, because the fragmented eastern flank has been subducted. The final episode of plate fragmentation occurred at the beginning of the Miocene, when the Cocos plate was split off, leaving the much reduced Farallon plate to be renamed the Nazca plate, and initiating Cocos–Nazca spreading. Some Oligocene Farallon plate with rifted margins that are a direct record of this plate-splitting event has survived in the eastern tropical Pacific, most extensively off northern Peru and Ecuador. Small remnants of the conjugate northern rifted margin are exposed off Costa Rica, and perhaps south of Panama. Marine geophysical profiles (bathymetric, magnetic and seismic reflection) and multibeam sonar swaths across these rifted oceanic margins, combined with surveys of 30–20 Ma crust on the western rise-flank, indicate that (i) Localized lithospheric rupture to create a new plate boundary was preceded by plate stretching and fracturing in a belt several hundred km wide. Fissural volcanism along some of these fractures built volcanic ridges (e.g., Alvarado and Sarmiento Ridges) that are 1–2 km high and parallel to “absolute” Farallon plate motion; they closely resemble fissural ridges described from the young western flank of the present Pacific–Nazca rise. (ii) For 1–2 m.y. prior to final rupture of the Farallon plate, perhaps coinciding with the period of lithospheric stretching, the entire plate changed direction to a more easterly (“Nazca-like”) course; after the split the northern (Cocos) part reverted to a northeasterly absolute motion. (iii) The plate-splitting fracture that became the site of initial Cocos–Nazca spreading was a linear feature that, at least through the 680 km of ruptured Oligocene lithosphere known to have avoided subduction, did not follow any pre-existing feature on the Farallon plate, e.g., a “fracture zone” trail of a transform fault. (iv) The margins of surviving parts of the plate-splitting fracture have narrow shoulders raised by uplift of unloaded footwalls, and partially buried by fissural volcanism. (v) Cocos–Nazca spreading began at 23 Ma; reports of older Cocos–Nazca crust in the eastern Panama Basin were based on misidentified magnetic anomalies.

There is increased evidence that the driving force for the 23 Ma fission of the Farallon plate was the divergence of slab-pull stresses at the Middle America and South America subduction zones. The timing and location of the split may have been influenced by (i) the increasingly divergent northeast slab pull at the Middle America subduction zone, which lengthened and

* Fax: +1 858 534 6849.

E-mail address: plonsdale@ucsd.edu.

reoriented because of motion between the North America and Caribbean plates; (ii) the slightly earlier detachment of a northern part of the plate that had been entering the California subduction zone, contributing a less divergent plate-driving stress; and (iii) weakening of older parts of the plate by the Galapagos hotspot, which had come to underlie the equatorial region, midway between the risecrest and the two subduction zones, by the Late Oligocene.

© 2005 Elsevier B.V. All rights reserved.

Keywords: Rifted margins; Plate formation; Plate motions; Lithospheric rupture

1. Introduction

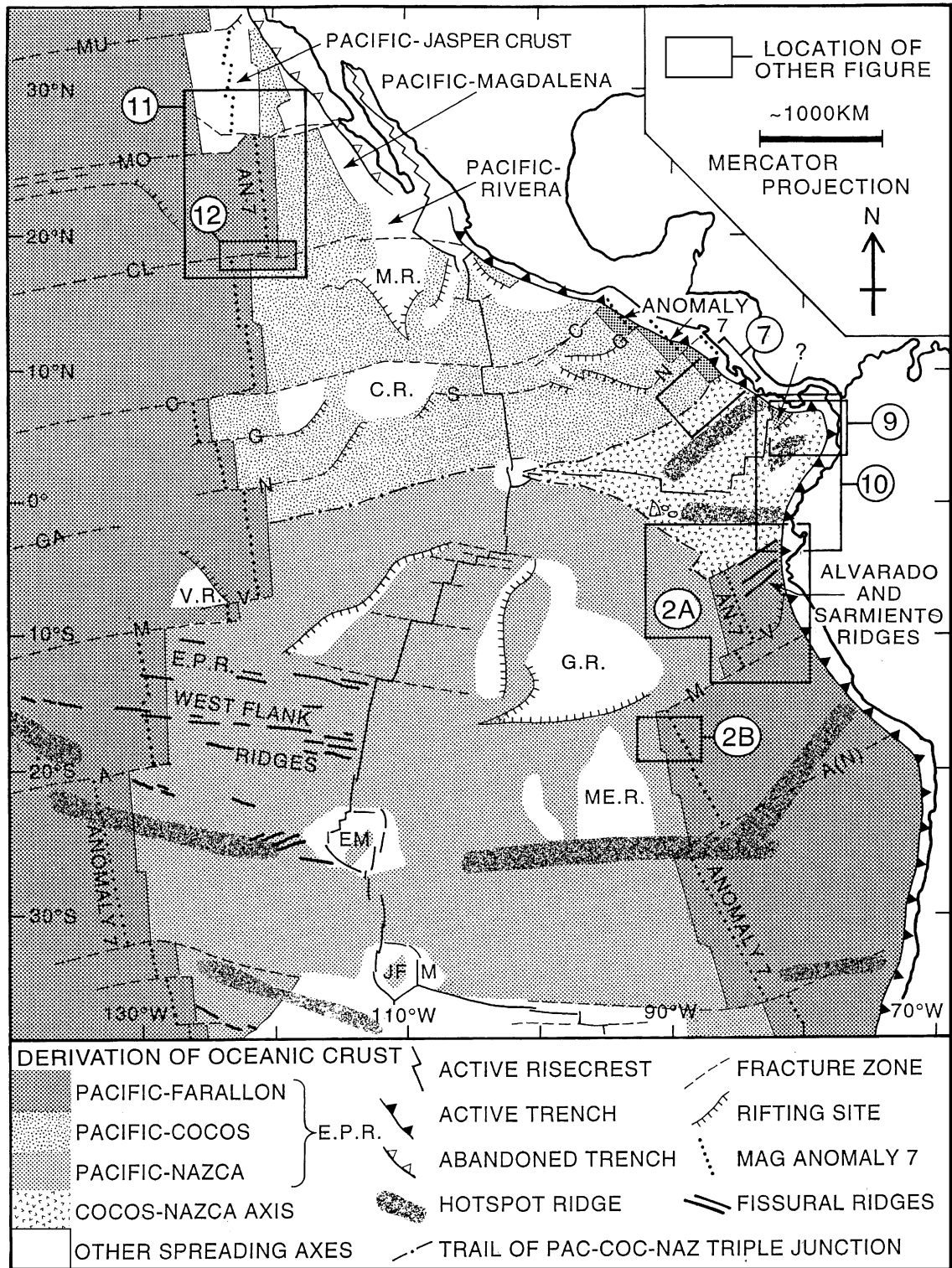
One of the most important events establishing the modern plate geography of the eastern tropical Pacific was the split of the oceanic Farallon plate into Cocos and Nazca plates at the beginning of the Miocene. Far-reaching consequences included acceleration of spreading on the East Pacific Rise (EPR), where Lower Miocene spreading was at world-record speeds (e.g., Wilson, 1996); changes in EPR spreading direction, altering its segmentation pattern and spawning the growth of risecrest microplates (e.g., Goff and Cochran, 1996); and faster, less oblique subduction at trenches along the western margins of the North American, Caribbean, and South American plates, changing volcanic and tectonics processes there (e.g., Sigurdsson et al., 2000; Sempere et al., 1990). The split was not unprecedented, for northern parts of the Farallon plate had split away as the Vancouver and Monterey plates in the Eocene and Oligocene (Menard, 1978; Atwater, 1989), and a similar process recurred later in the Miocene, as other independently moving plates (e.g., Magdalena, Rivera) were detached from the Cocos plate (Lonsdale, 1991). However, there is no evidence that any of these other episodes in the complex history of Farallon plate fragmentation gave birth to new spreading centers between diverging fragments, whereas a new Cocos–Nazca (C–N) spreading center was a major, persisting result of the Early Miocene split. Admittedly, in all the other cases the intra-plate fractures that developed

into plate boundaries have been lost to subduction, so their natures and patterns are conjectural; the survival of parts of the original fractures that developed into the initial C–N boundary makes this split the most amenable to investigation.

Previous studies of the C–N split, seeking insight into the integrity, strength and dynamics of oceanic plates and the origin of spreading centers, or just trying to unravel the regional geologic history, have examined where, when, how and why it happened. This paper uses new data to reopen these questions, and come up with some new answers.

Handschumacher (1976) and Hey (1977) located one piece of the original plate-splitting fracture at Grijalva Scarp, a northeast-striking topographic step on the Nazca plate that is still 680 km long, despite being subducted at 80 km/m.y. in the trench off Ecuador. The scarp now separates the oldest C–N crust from still older EPR (Pacific–Farallon) crust. At its southwestern end it meets a more subdued crustal boundary, the Nazca-plate trail of the Pacific–Cocos–Nazca triple junction, which separates C–N crust from coeval Pacific–Nazca crust. Hey (1977) could find no surviving trace of a conjugate to Grijalva Scarp on the Cocos plate (he supposed that the Cocos-plate trail of the triple junction now extends all the way to the Middle America subduction zone), but did speculate that part of the hypothetical scarp, referred to here as Hernando Scarp after the Spanish explorer Hernando de Grijalva, could have avoided fast Cocos plate subduction if it had been captured by the Nazca plate, and may

Fig. 1. Present structural pattern of the eastern tropical Pacific, locating the charts of Figs. 2, 7, 9, 10, 11 and 12 and the divergent plate boundaries that accreted extant oceanic crust. Note the large (white) areas accreted at the margins of microplates, on the crests of microplate rises (M.R.=Mathematician Ridge, C.R.=Clipperton Rise, V.R.=Viru Rise, G.R.=Galapagos Rise, ME.R.=Mendoza Rise); EM and JFM are the Easter and Juan Fernandez microplates. Fracture zone abbreviations are MU=Murray, MO=Molokai, CL=Clarion, C=Clipperton, G=Guatemala, N=Nicaragua, GA=Galapagos, V=Viru, M=Marquesas (west flank) and Mendana (east flank), A(N)=Austral (west flank), Nazca (east flank).



survive in the basin immediately south of the Isthmus of Panama. Lonsdale and Klitgord (1978) suggested that the captured part of Hernando Scarp obliquely crosses the uplifted crust of Coiba Plateau, then follows the foot of the Panamanian continent slope, in part forming the “South Panama Boundary Ridge” of Westbrook et al. (1995). Survival of an uncaptured 75-km length of Hernando Scarp, still on the Cocos plate at the outer rise of the Middle America Trench off Costa Rica, was reported by Massell and Lonsdale (1997) and Meschede et al. (1998). I describe the variable structure of Hernando Scarp off Costa Rica and reassess the evidence for captured fragments south of Panama.

A minimum age for the split into Cocos and Nazca plates can be obtained by dating the oldest C–N crust. Handschumacher (1976) and Lonsdale and Klitgord (1978) found that the crest immediately northwest of Grijalva Scarp accreted during magnetic Chron 6B (23.1–22.6 Ma). Magnetic mapping southeast of Hernando Scarp off Costa Rica (Barckhausen et al., 2001) gives the same result. Analyses of the changing orientation of magnetic stripes and abyssal hills on the flanks of the southern EPR (e.g., Handschumacher, 1976; Lonsdale, 1989; Searle et al., 1995) demonstrated that the southern half of the northeast-moving Farallon plate began to veer toward the more easterly motion of the future Nazca plate well before Chron 6B, but new data from the northern EPR flanks show that the northern half also started moving eastward, before reverting to a northeasterly “Cocos” course. I infer that an intact Farallon plate began to veer to a more easterly (“Nazca”) motion, and then fissioned, first by diffuse extension in a mid-plate band several hundred kilometers wide, then by focused C–N separation at a Chron 6B spreading center.

Handschumacher (1976), Hey (1977), Lonsdale and Klitgord (1978) and Barckhausen et al. (2001) followed Mammerickx et al. (1975) in assuming that the Grijalva Scarp rifting site was originally a Farallon plate fracture zone, the east-flank trail of a transform on the Pacific–Farallon EPR (perhaps the Galapagos transform, even though Handschumacher (1976) and Mammerickx and Klitgord (1982) noted that Grijalva Scarp is further south than the expected east flank trail of this transform). Splitting the Farallon plate along a risecrest-to-trench fracture zone seemed consistent with the notion that such features represent inherited

zones of weakness within oceanic plates. My new analysis indicates that neither Grijalva Scarp nor most of the other eruptive fractures on surviving parts of the Farallon plate coincide with preexisting fracture zones. At 25–23 Ma there were no risecrest-to-trench fracture zones across the central, rupturing part of the plate, for a distance of 1900 km between Clipperton and Mendana fracture zones. All of the Clipperton fracture zone that crossed the Farallon plate at that time has been lost to subduction (no east-flank EPR crust older than 17 Ma remains on the north side of this fracture zone). A several hundred km length of the contemporary Mendana fracture zone does survive west of the Peru–Chile Trench, and its breadth and tectonic complexity have been taken as evidence that this fracture zone has been a site of mid-plate rifting (Warsi et al., 1983), but, as discussed below, the timing of any such rifting is controversial.

As for what caused the Farallon plate to split apart in its equatorial region at the beginning of the Miocene, suggestions have included (1) a build-up of intra-plate extensional stress from the divergent slab pulls of the differently oriented Middle America and South America trenches (Lonsdale and Klitgord, 1978; Wortel and Cloetingh, 1981) and (2) birth of the Galapagos hotspot (Hey, 1977).

This paper’s revised interpretations of where, when and how the Farallon plate split are based on analysis of magnetic profiles, multibeam bathymetry swaths, and some single-channel seismic reflection profiles in three areas located in Fig. 1 (west of Peru, south of Panama, and southwest of Costa Rica), and on the patterns of EPR fracture zones mapped by multibeam bathymetry and satellite altimetry. After presenting these interpretations, I reopen discussion of why the Farallon plate split when and where it did.

2. Evidence from west of Peru

2.1. Grijalva scarp and ridge

A change in regional depth between the Peru Basin and the younger, shallower Carnegie Platform marks the most extensive surviving boundary between EPR crust that accreted to the Farallon plate before it split apart, and C–N crust that accreted afterwards. This “Grijalva Scarp” has not been systematically swath-

mapped, but its pattern and structural setting (Fig. 2) are defined by many bathymetric and magnetic profiles, and by satellite altimetry (Sandwell and Smith, 1997) along its high-relief portion. A few single-channel seismic reflection traverses (e.g., Figs. 3 and 4) help resolve its local structure, though their value is

diminished by the prevalence of a Miocene chert horizon (sampled at Deep Sea Drilling Project [DSDP] Site 157 (Van Andel et al., 1973)) that creates a flat-lying acoustic basement for much of the Carnegie Platform. Even more valuable are a handful of multibeam bathymetric traverses, including those near

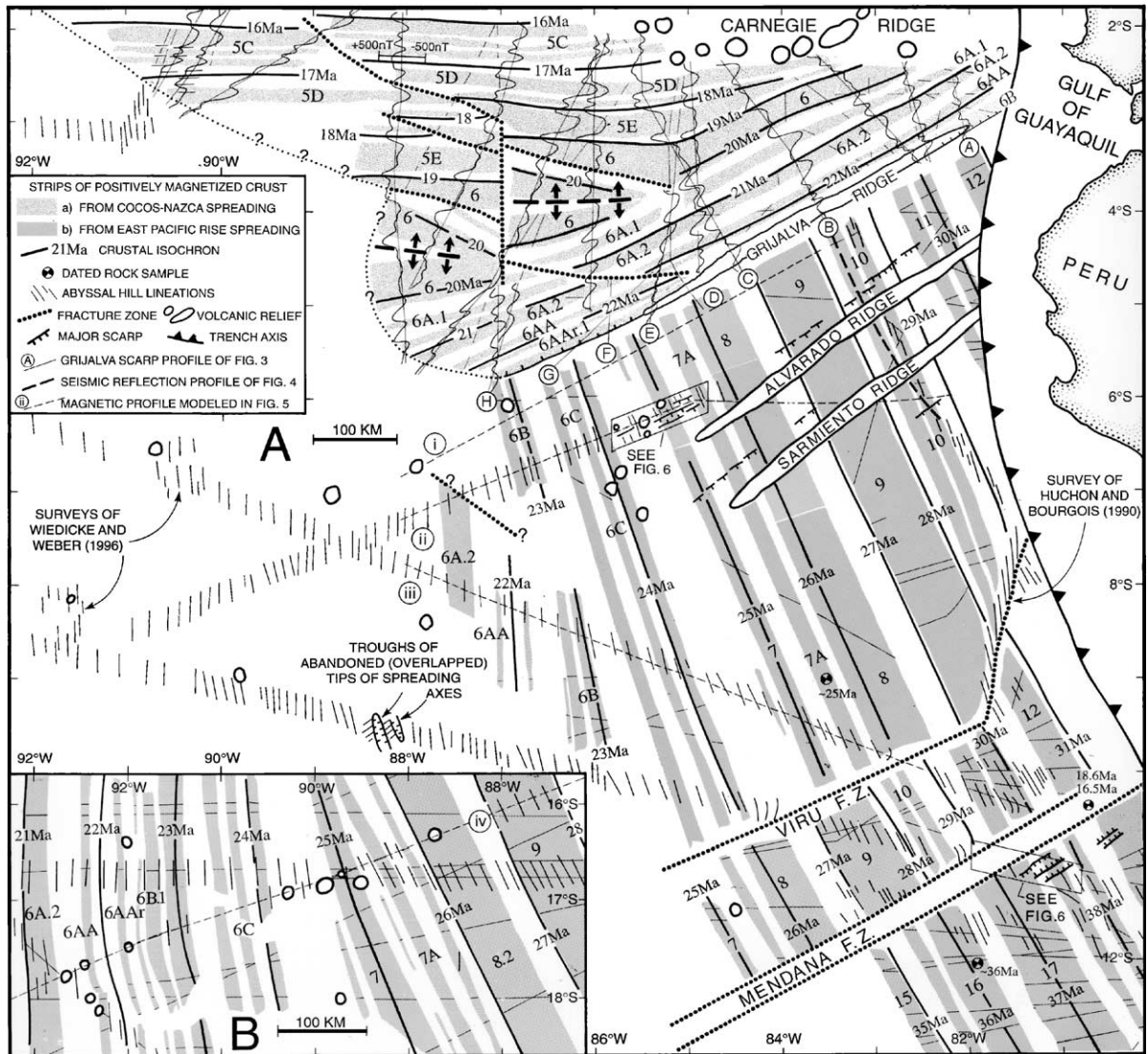
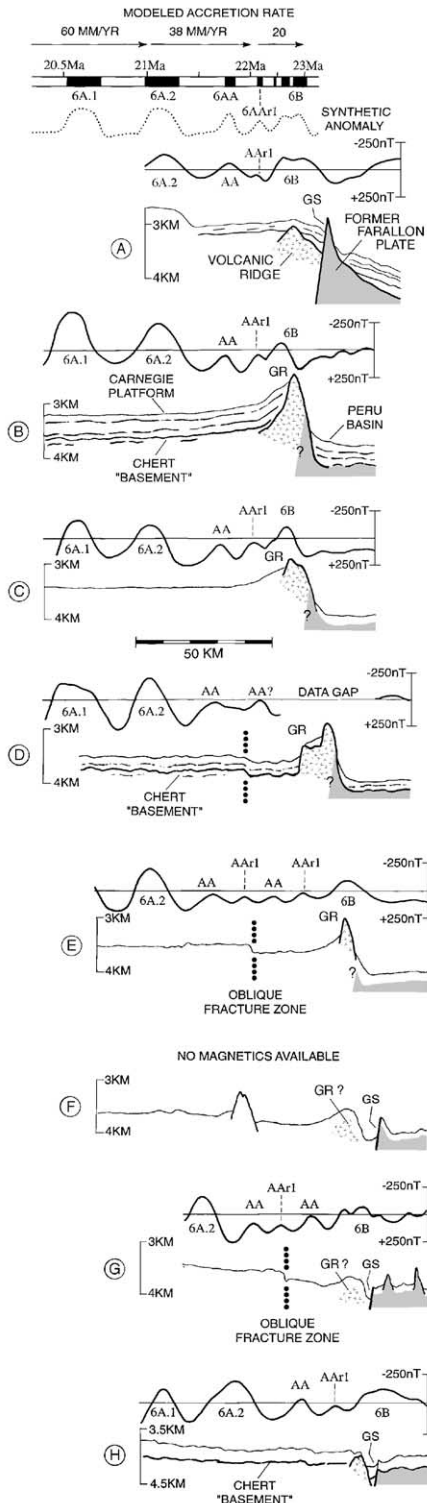


Fig. 2. Reinterpretation of magnetic lineations west of Peru, based on archival magnetic profiles, and the azimuths of abyssal hills mapped along multibeam sonar swaths. Magnetic profiles i–iv are modeled in Fig. 5 to justify the identification of EPR stripes. Thin solid lines across the magnetic stripes locate other magnetic profiles used in this interpretation but not displayed in this figure. At latitudes of 2°S–10°S, abyssal hill lineations indicate that Pacific–Nazca magnetic stripes would strike almost north–south; at these latitudes these magnetic anomalies cannot be identified because of their very low amplitude, and the high noise level from the equatorial electrojet. Insert B shows the pattern of readily identified stripes at higher latitudes, where there is a better record of the changing azimuth of the EPR spreading center during the Farallon to Nazca transition.



longitude 82°W and 83.5°W collected with the high-resolution broad-swath Simrad EM-120 sonar (Fig. 4).

The age of Peru Basin crust on the older side of the Grijalva lineament decreases from more than 31 Ma at the trench to 23 Ma where its southwestern end intersects EPR Anomaly 6B (Figs. 2 and 5). The age of Carnegie Platform crust on its younger side is a constant 23 Ma (Fig. 3). Where the age-difference across the lineament is less than 2 Myr, i.e., for 160 km near its southwestern end, the relatively low relief (Fig. 3, profiles F–H) includes a 100–400 m-high fault scarp along the northwest side of a locally uplifted shoulder of EPR crust. A trough along the foot of the northwest-facing scarp is bounded on the northwest by a low volcanic (?) ridge of C–N crust. A similar arrangement of northwest-facing fault scarp with a sediment-covered ridge at its foot also exists along ~75 km of the other, northeastern, end of the lineament, where it separates crust with an age-difference of 7.5–8.5 Myr as it obliquely descends the outer slope of the Ecuador Trench. The buried ridge in this region, which follows C–N magnetic anomaly 6B, is well portrayed on the seismic reflection profile of Fig. 3A, and the adjacent scarp with its rift shoulder of uplifted EPR crust is imaged by the concurrently collected multibeam bathymetry swath at 82° (Fig. 4). This well developed fault scarp on the trench slope may not be entirely a relic of Early Miocene plate fission; the plate-splitting fracture may have been rejuvenated by recent subduction-related tectonism. As noted by Gutscher et al. (1999), seismicity indicates that the subducted slab beneath southern Ecuador, inferred to be former Farallon lithosphere, has a much steeper dip than the slab below central Ecuador, inferred to be younger lithosphere accreted by C–N spreading and crust-thickening hotspot volcanism; they suggest that the downgoing slab tears along the subducted extension of the Grijalva lineament. Perhaps the tear extends seaward of the trench axis, across an exposed part of the plate, with normal faulting accommodating the differing response of the

Fig. 3. Interpreted bathymetric, seismic reflection and magnetic profiles projected northwest–southeast normal to the 060° strike of Grijalva Ridge (GR) and Grijalva Scarp (GS), located in Fig. 2. Northwestern limit of (shaded) Farallon Plate crust is hypothetical for profiles B–E, where the boundary has been smothered by Grijalva Ridge volcanism.

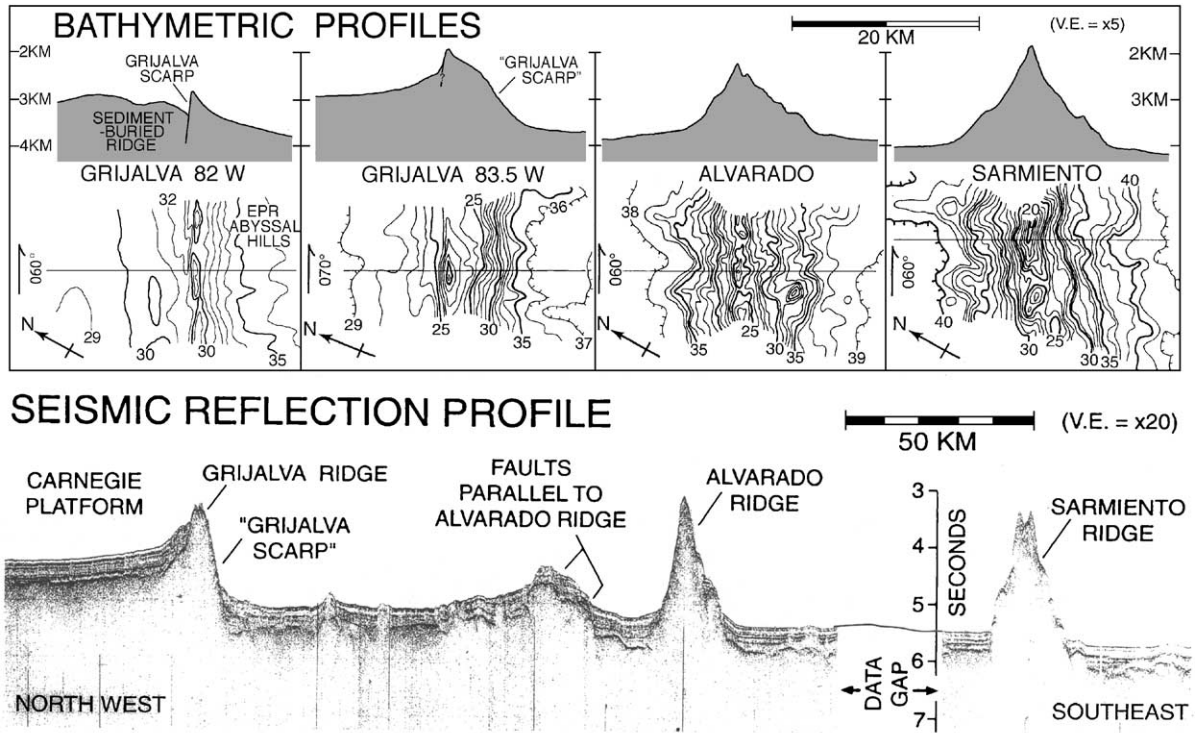


Fig. 4. A single channel seismic reflection profile at 83.5–83°W (partly sketched as profile B of Fig. 3) across the three volcanic ridges of the rifted margin of the Farallon plate off northwestern Peru. Multibeam bathymetry from a Simrad EM-120 sonar is shown by contour swaths at 100 m vertical interval, and by center-beam profiles. These swaths were collected along almost the same line as the seismic reflection profile, and across Grijalva Scarp at 82°W (Fig. 3, profile A) on the outer slope of the Ecuador Trench.

two types of lithosphere to different rates of plate bending. A greater bending moment applied to the more steeply dipping EPR-derived part of the slab may cause greater flexural uplift of the outer-slope crust to the southeast of the Grijalva lineament.

Linking the two segments where a northwest-facing fault scarp (labeled Grijalva Scarp in Fig. 3) marks the rifted margin of Farallon lithosphere, a 450 km length of the plate fission site is occupied by a partly outcropping 10–15 km-wide basement ridge with a crest at least 1 km shallower than the acoustic basement of the Carnegie Platform. This Grijalva Ridge is aligned with the lower sediment-covered scarp-foot ridges to the southwest and northeast, and with a high-amplitude magnetic anomaly that is continuous along-strike and identified as Anomaly 6B (Fig. 3). It is inferred to be mainly the product of voluminous fissure eruptions that in the initial stage of C–N spreading built a volcanic ridge higher than any adjacent rift scarp, and partly or completely buried any

rift-shoulder uplift of 2–7.5 Myr-old (now 25–30.5 Ma) Farallon lithosphere. Evidence that a volcanic Grijalva Ridge was buttressed on its southeast side by a footwall uplift of older rifted EPR crust comes from upslope–downslope lineations resembling EPR abyssal hills on the lower part of the southeast-facing slope at the 83.5°W transect (Fig. 4). This high slope overlooking the Peru Basin was named Grijalva Scarp by Mammerickx et al. (1975), and is labeled “Grijalva Scarp” in Fig. 4, but its modest (<20°) inclination and fine-scale morphology (e.g., on the multibeam swath at 83.5°W of Fig. 4) indicate that the slope is not the scarp of a southeast-dipping fault.

Grijalva Ridge has a large-amplitude gravity anomaly that allows delineation of its regional pattern by satellite altimetry. It has an overall strike of 060°, so it truncates EPR magnetic stripes of Chrons 7A to 12, which have an average strike of 335° (Fig. 2), at an angle of 095°, rather than orthogonally. Altimetry indicates that the ridge is straight except for a 15–20

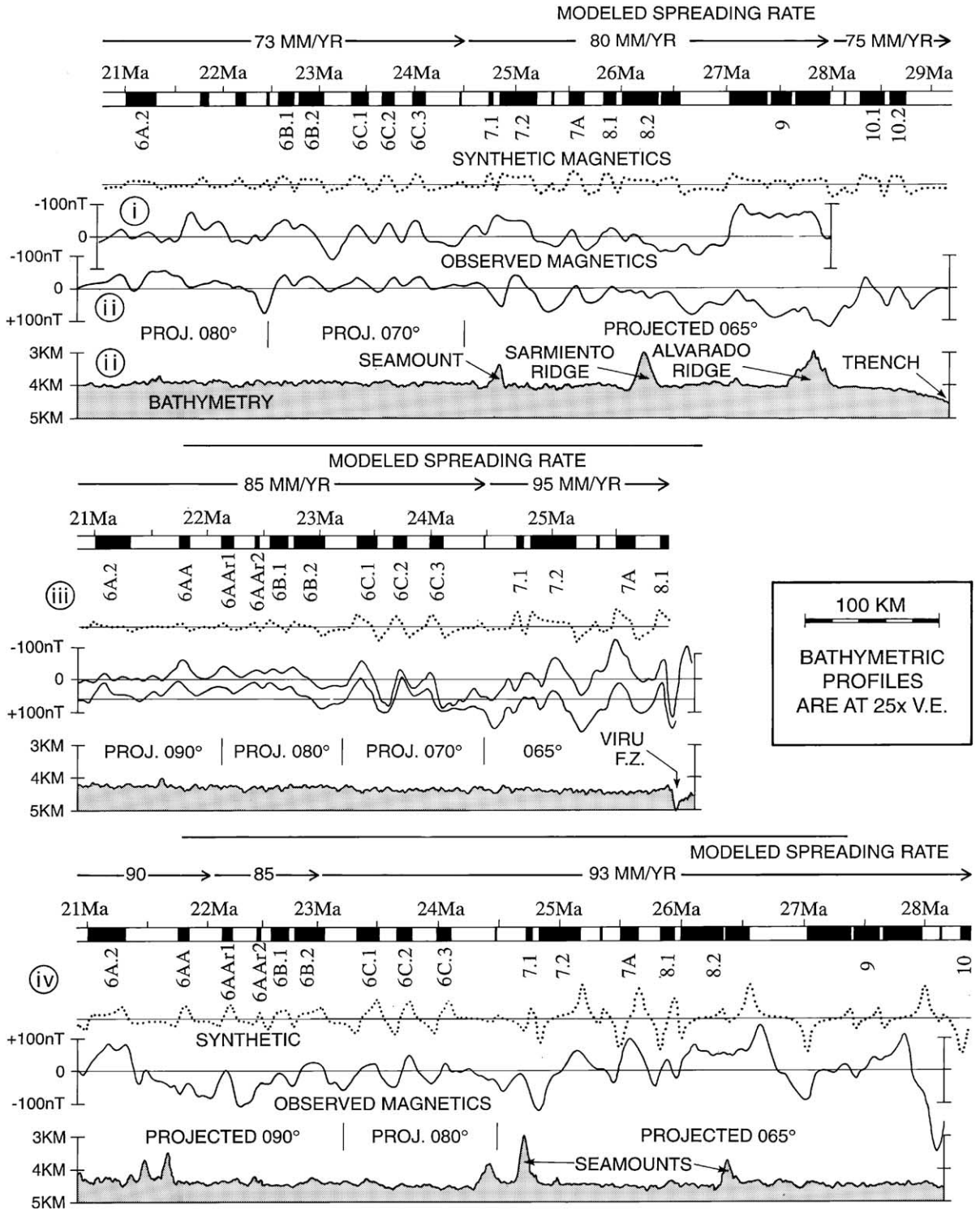


Fig. 5. Observed and modeled magnetic anomalies along four profiles plotted in Fig. 2. No bathymetry is available for profile I; for iii two almost collocated magnetic profiles (less than 3 km apart) are shown.

km left step or kink near 84.8°W, but at some multi-beam traverses (e.g., at 83.5°W, Fig. 4) the local strike of the ridge is 070°, suggesting there may be an echelon ridge segments separated by additional left steps that are too short to resolve with altimetry.

Magnetic anomaly patterns indicate that spreading between Cocos and Nazca plates began along the entire extant length of the Grijalva rifting site during Chron 6B (23.1–22.6 Ma according to the timescale of Cande and Kent (1995) that is used throughout this paper). For its first 2 m.y. the new spreading center stayed parallel to the initial northeast-striking rift, with its only identifiable offset originating at and migrating westward away from the small left step of the rift at 84.8°W. This pattern may imply that early C–N spreading was normal to the rift, and this is the assumption used in Fig. 3 to estimate the south-flank rate of crustal accretion (accelerating to 38 mm/yr by 22 Ma and 60 mm/yr by 21 Ma). The alternative interpretation is that the early C–N axis spread faster, but obliquely (e.g., north–south). After 3 m.y. of C–N spreading, the western part of the axis began reorienting to an east–west strike that is inferred to be normal to the post-20 Ma spreading direction, because there is evidence for a north–south transform fault near 87°W. East of 85°W the spreading center maintained a northeasterly strike, presumably with oblique north–south spreading, for another 1–2 m.y. (Fig. 2). Reorientation of spreading axes west of 85°W was accompanied by the development of westward-migrating nontransform offsets, and by abandonment of spreading segments that were overlapped by propagating rifts. These processes left a pattern of magnetic stripes on the Carnegie Platform that is complex and not fully resolved by available data; a slightly different interpretation was presented by Barckhausen et al. (2001). The arrangement of oblique fracture zones and abandoned spreading axes mapped in Fig. 2 is partly hypothetical, but is consistent with bathymetry, seismic reflection profiles and satellite altimetry as well as with the widely spaced magnetic profiles.

2.2. Other rifting sites in the Farallon plate

Alvarado and Sarmiento Ridges are 1–2 km high, 400 km-long volcanic ridges, which strike 050–055° across the Peru Basin 150 km and 250 km southeast

of Grijalva Ridge (Fig. 2). They are similar to that ridge in extending from the trench to about the 25 Ma EPR isochron; they are different in (still) being surrounded by EPR crust. Though they were originally interpreted as fracture-zone traces of transform faults on the Pacific–Farallon EPR (Mammerickx et al., 1975), they do not offset magnetic stripes, nor even cross them orthogonally. Based on the available data, which include a few traverses of multibeam bathymetry (e.g., Fig. 4), but no analyses of rock samples, these ridges most closely resemble the linear volcanic ridges built over eruptive fractures that extend down the young flanks of active eastern Pacific rises, such as Sojourn Ridge on the Pacific–Nazca EPR (Cormier et al., 1997).

The abyssal hill fabric of the northeastern Peru Basin is also disrupted by extensional faulting along non-eruptive fractures. Prominent fault scarps occur alongside the volcanic ridges (e.g., 25 and 35 km north of Alvarado Ridge on the profile of Fig. 4), and extend into slightly younger crust further west on the EPR flank, as on the Seabeam 2112 swath A of Fig. 6, where scarps that strike 060°–065° have almost orthogonal intersections with abyssal hill lineations.

Mendana fracture zone, 800 km southeast of Grijalva Ridge (Fig. 2) has been identified as another site of plate splitting. Warsi et al. (1983) based this interpretation on the great width of the eastern part of the fracture zone and its apparent broadening toward the trench. They inferred, despite the lack of recorded seismicity, that rifting normal to the trench was still continuing along at least 400 km of the fracture zone. This inference was supported by Huchon and Bourgois (1990); indeed, their marine geophysical survey led them to propose that trench-parallel seafloor spreading between two old parts of the Nazca plate separated by Mendana fracture zone began about 3.5 Ma and was still active. This proposition was disproved by subsequent recovery from within 5 km of the supposed “spreading axis” of altered ferromanganese-encrusted basalt that yielded minimum ages, by K–Ar dating, of 18.6, 16.5, and 12.2 Ma (Bourasseau et al., 1993).

High resolution multibeam bathymetry of this eastern part of Mendana fracture zone (e.g., Fig. 6, swath B) shows that much of its great width, as at many other large Pacific fracture zones (e.g., Searle, 1983), is explained by its segmentation into multiple strands

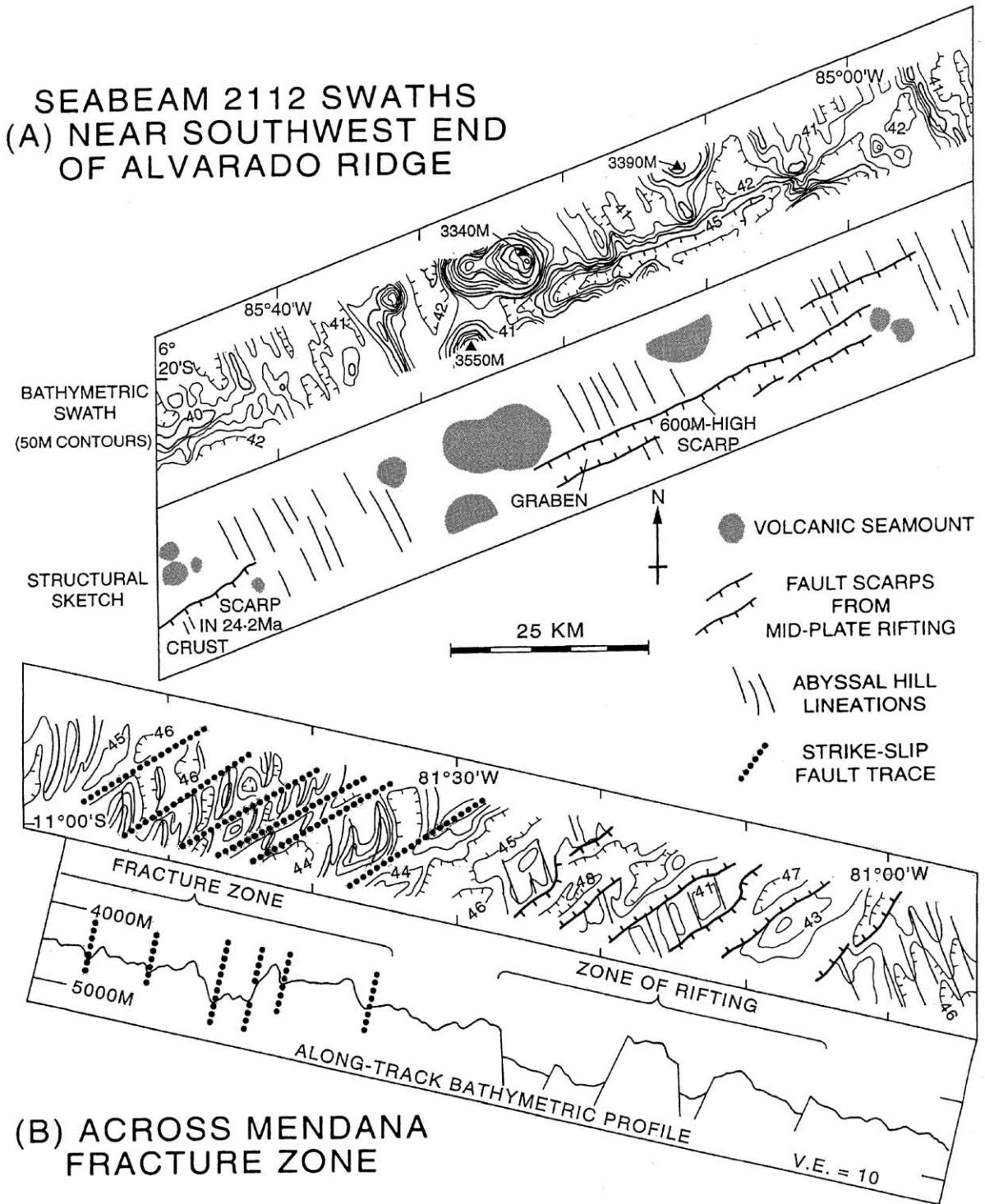


Fig. 6. Bathymetry plus structural interpretation of two Seabeam 2112 multibeam swaths, located in Fig. 2.

separated by short, characteristically oblique or sigmoidal abyssal hills on crust that spread from short intra-transform spreading axes. About 50 km of its width is thus explicable as an inheritance from the complex but not atypical segmentation of this part of the Oligocene Pacific–Farallon plate boundary. On the older southeastern side of the fracture zone there is an almost equally broad belt of high-relief ridges and troughs which cut normal abyssal hill terrain, and do seem to denote later extensional faulting of lithosphere that accreted adjacent to but outside the segmented transform fault system. Within the survey of Huchon and Bourgois (1990), in the “old fracture zone” region of their Fig. 3, the fault scarps defining these troughs strike about 10° oblique to the 060° strike of the fracture zone.

It is possible that the extensional faulting of the 37–40 Ma lithosphere on the southeast side of Mendana fracture zone dates from the 25–23 Ma stretching and splitting of the Farallon Plate. The K/Ar analyses of the lavas collected within the fracture zone from volcanic ridges that strike 060° , parallel to Grijalva Ridge, do not preclude their eruption during the same period. It is, however, equally plausible that the observed structures of the fracture zone were simply inherited from the Oligocene Pacific–Farallon Mendana transform and were unaffected by any subsequent Farallon (or Nazca) plate split. Transform-parallel and oblique fault troughs that originate in the inside corner between spreading axis and transform fault, and end up on the older side of rise-flank fracture zones, are features of large Pacific transforms that have experienced small extensional changes in the direction of relative plate motion (Lonsdale, 1994). Some such transforms have ridge-building volcanism along their strike-slip fault segments (e.g., Hekinian et al., 1992; Perfit et al., 1996), characteristically erupting primitive basalt derived from picritic melts, like some of the Mendana lavas described by Bourasseau et al. (1993).

3. Evidence from southwest of Costa Rica

An abrupt crustal boundary that is the Cocos-plate conjugate of the southwestern part of Grijalva Scarp crosses the thickly sedimented outer slope of the Middle America Trench seaward of the Nicoya Pen-

insula (Fig. 7). To the northwest of this Hernando Scarp, crust that accreted to the Farallon plate at 60 mm/yr during Chron 6C is lineated parallel to a straight section of the trench axis; trench-parallel normal faults (Shipley and Moore, 1986) are abyssal-hill boundary faults rejuvenated by flexural extension of the upper lithosphere as it bends into the subduction zone. Subducting Pacific–Farallon crust immediately northwest of Hernando Scarp has been intensively studied by multibeam surveys and single-channel seismic profiling (Shipley and Moore, 1986), three-dimensional multichannel profiling (Shipley et al., 1992), submersible dives (McAdoo et al., 1996), and deep drilling during Ocean Drilling Program (ODP) Leg 170 (Kimura et al., 1997). It is magnetically dated at 24 Ma (Fig. 7), though oceanic “basement” sampled at ODP Site 1039 is a gabbroic intrusion into Middle Miocene (16 Ma) sediment, indicative of mid-plate magmatism. Crust immediately southeast of Hernando Scarp has magnetic stripes that are almost orthogonal to the trench axis, and to the recently created graben-bounding faults produced by bending-induced faulting of the outer slope (where abyssal hill lineations are difficult to resolve because of the 300–400 m-thick sediment blanket). This crust was accreted at a C–N spreading axis, beginning about 23 Ma (Chron 6B), with a “half spreading rate” (assuming orthogonal spreading) that had increased to 29 mm/yr by 22 Ma (Fig. 8). Younger C–N crust further southeast, which is overprinted with volcanic outliers of the Cocos Ridge hotspot trail (von Huene et al., 1995), was accreted by a 19–17 Ma spreading axis that had rotated 20° clockwise from its original strike (Fig. 7). Absence off Costa Rica of crust representing much of the 21–19 Ma interval indicates that this rotation was accompanied by rift propagation which transferred crust to the southern flank of the C–N rise, where it survives on the northern flank of abandoned spreading axes (Fig. 2). The shift in C–N stage poles at 19.5 Ma is just the first of many, often accompanied by reorganization of the accreting plate boundary (Wilson and Hey, 1995), that have been precipitated by the frequently changing motions of the Cocos and Nazca plates throughout the Neogene. Barckhausen et al. (2001) refer to the pre-19.5 Ma and post-19.5 Ma “episodes” of C–N spreading as CNS-1 and CNS-2, and from their identification of the northeast-striking CNS-1 anoma-

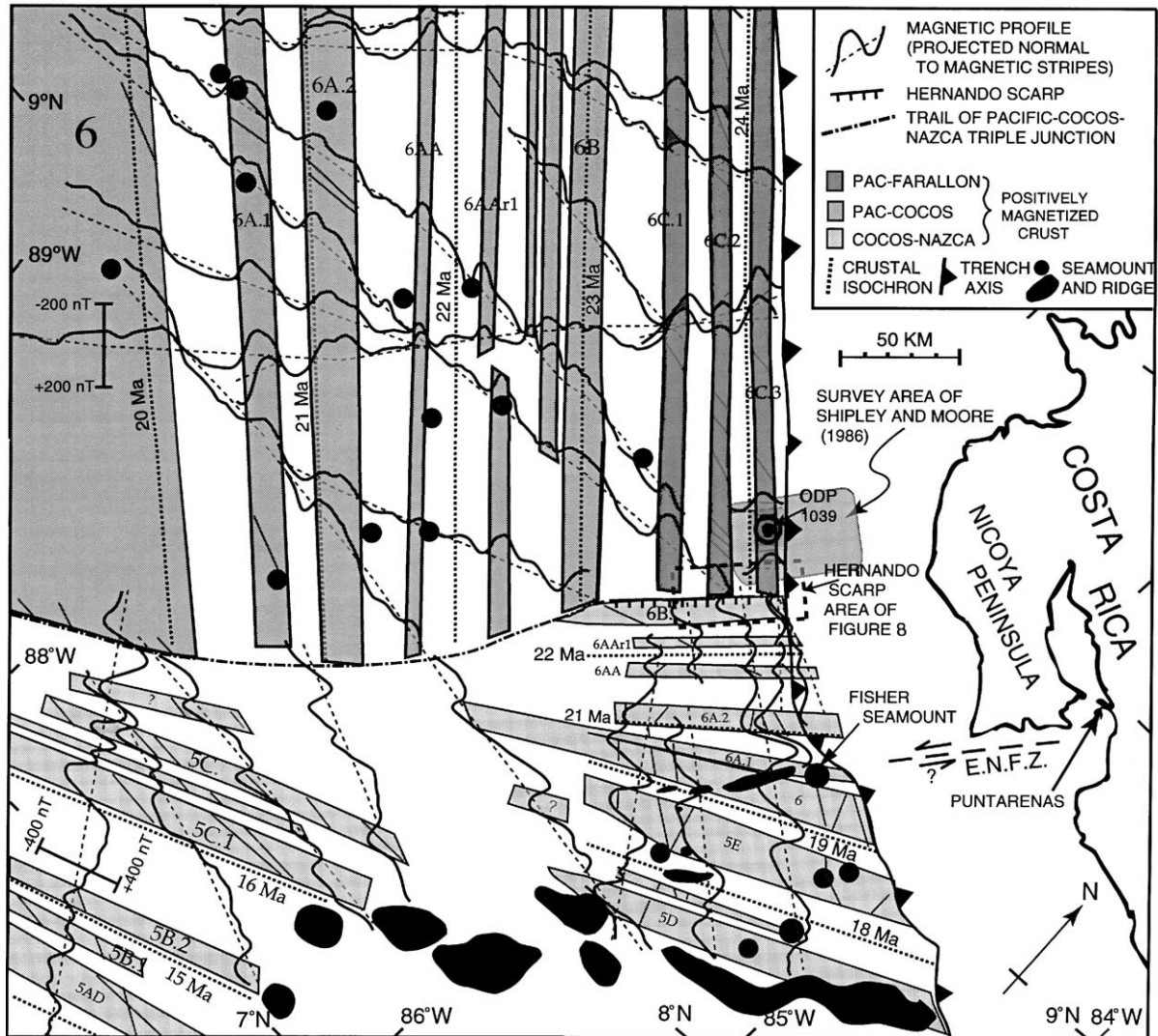


Fig. 7. Interpretation of magnetic stripes off Costa Rica (located in Fig. 1), showing the regional context of the plate rifting site along Hernando Scarp. Note that the lower amplitude magnetic anomalies on EPR (Pacific–Farallon and Pacific–Cocos) crust are displayed at a different scale than those on Cocos–Nazca crust. Thin solid lines across the magnetic stripes locate other magnetic profiles used in this interpretation, but not displayed in this figure. “E.N.F.Z.” is the East Nicoya fault zone that Protti et al. (1995) mistakenly thought to be aligned with the EPR/C–N Rise boundary.

lies they reach the remarkable conclusion that the initial rate of north-flank C–N spreading was 50 mm/yr, faster than any subsequent north-flank rate. This difference from my interpretation of a gradual acceleration of early C–N spreading, on both the north flank (Figs. 7 and 8) and south flank (Fig. 3), is based on their identifying as 6AAr.1 the anomaly I model as 6AA (Fig. 8).

The 40 km of Hernando Scarp on the outer slope of the trench were completely swath-mapped by a Seabeam 2112 sonar, and these results from our survey were used in the regional bathymetric mapping of von Huene et al. (2000). On the upper slope (e.g., profile C, Fig. 8) the crustal boundary is marked by a south-east-facing fault scarp as high as 300 m, with the structural relief of faulted basement being probably

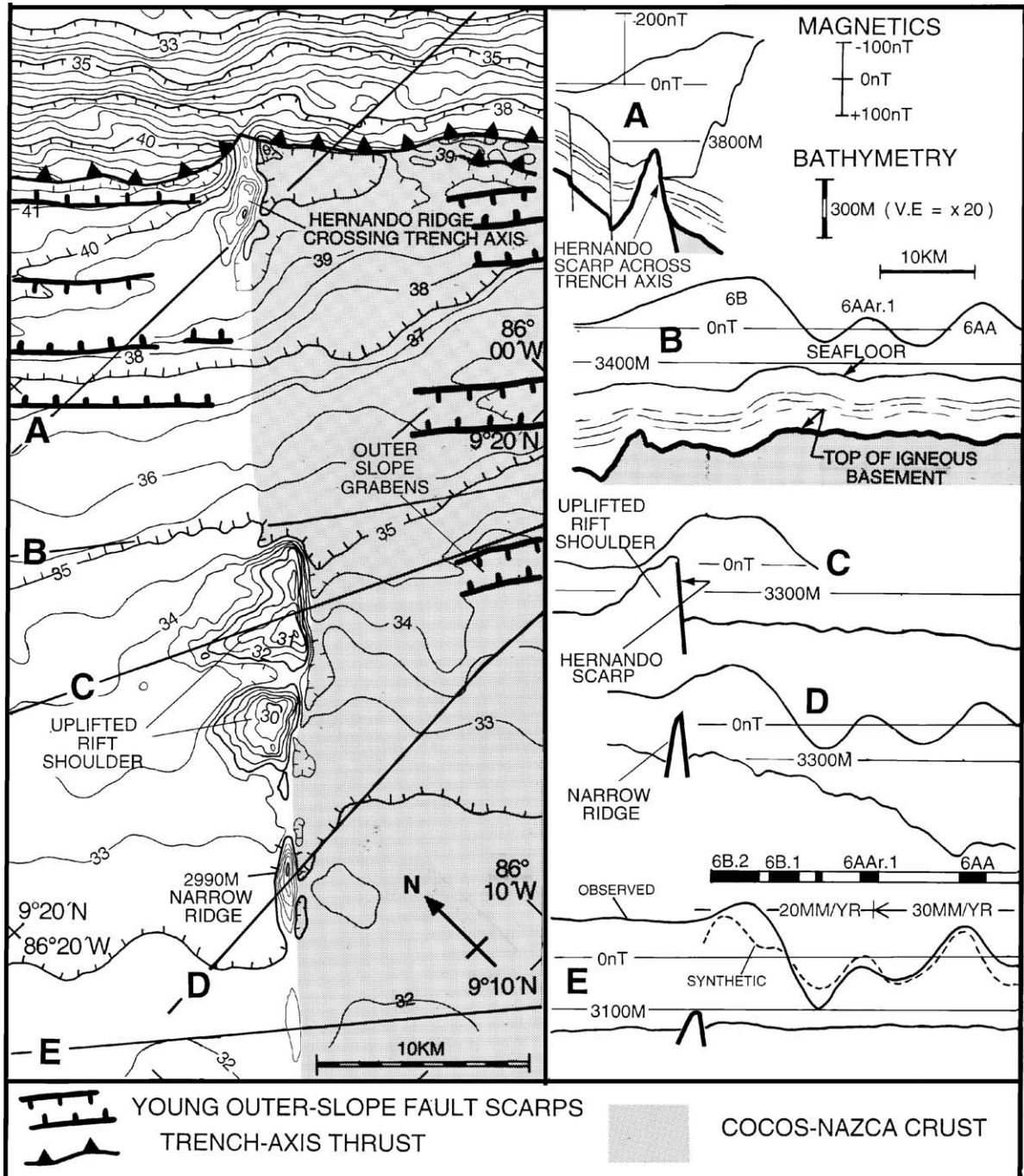


Fig. 8. Multibeam bathymetry of Hernando Scarp on the outer slope of the trench off Nicoya, and interpreted bathymetric, magnetic and seismic reflection transects.

twice as great. Where best developed (Profile C, Fig. 8), the fault scarp bounds a 10 km-wide rift shoulder of uplifted Chron 6C.2 crust that was once part of the Pacific–Farallon rise flank, and only ~0.5 Myr old at the time of rifting. At the bottom of the trench slope another segment of the narrow rift shoulder, with a scarp misaligned from the fault scarp of profile C by 2–3 km, is now entering the subduction zone (profile A, Fig. 8), crossing and slightly indenting the trench axis, and causing enough interruption to the north-west-deepening axial gradient that a small pond of turbidites has accumulated upstream. Its role in damming along-axis turbidity currents helps explain the absence of axial turbidities to the northwest, within the survey area of Shipley and Moore (1986). Between the trench-axis and upper slope segments of rift shoulder, the only bathymetric evidence for the crustal boundary is a slight (50–100 m) change in regional depth (shallower over the slightly younger C–N lithosphere to the southeast), and a gap in the young outer-slope fault scarps, between the two different regimes of bending-induced faulting. Profile B (Fig. 8) shows that on the mid-slope the basement relief of the crustal boundary has been completely smothered by pelagic sedimentation. At the top of the trench outer slope, the southwestern continuation of Hernando lineament across the outer rise is marked by a locally outcropping basement ridge that is sketched in profiles D and E (Fig. 8) as a very narrow uplifted rift shoulder, following interpretation by Barckhausen et al. (2001) of a low-resolution multichannel seismic reflection traverse. This region was within 40 km of the fast-spreading Pacific–Farallon axis at the beginning of Chron 6B, and an alternative explanation of this narrow ridge is that it is a volcanic construction, built by magma derived from axial upwelling that leaked into the rise-crest-intersecting plate-splitting fracture, as occurred on the present orthogonally split segments of EPR crest at 22.5°N (Lonsdale, 1995) and 55.6°S (Lonsdale, 1994).

The pattern of magnetic stripes (Fig. 7) indicates that the intersection of Pacific–Cocos and C–N Anomaly 6B, i.e., the beginning of the Cocos–Nazca–Pacific triple junction trail, occurs about 75 km southwest of the trench axis, at 9°N, 86.5°W. This site has not been surveyed with the seismic profiling and swath bathymetry needed to define the structural transition from a plate-splitting fracture

(along Hernando Scarp) to a triple junction trail; southwest of the area of Fig. 8 the next multibeam traverse that can precisely locate the crustal boundary by the juxtaposition of differently oriented abyssal hill lineations is near 88°W, 300 km from the trench. Widely spaced conventional sounding and profiler traverses indicate that this oldest part of the triple junction trail has low and sediment-smothered basement relief, unlike the rough rifted margins of the “Galapagos Gore” further west (Lonsdale, 1988).

The surviving length of Hernando Scarp, which Barckhausen et al. (2001) refer to as a “fracture zone”, is clearly conjugate to the southwestern end of Grijalva Scarp (e.g., at profiles D and F of Fig. 3), the part with a small difference in age and regional depth between rifted Pacific–Farallon crust and oldest C–N crust, and with much of the local relief from rift-shoulder uplift that creates a scarp facing the C–N axis. Because of its trench-crossing location, there may also be similarities to the northeastern end of Grijalva Scarp. The possibility exists that the normal faults at Hernando Scarp have recently been rejuvenated because of the different response to vertical bending (into the Middle America subduction zone) of the EPR and Cocos–Nazca lithosphere that the scarp separates.

As at the conjugate part of Grijalva Scarp, now located 1645 km almost due south because of 23 m.y. of C–N spreading, the overall trend of Hernando Scarp intersects Pacific–Farallon magnetic lineations at an angle of about 84°, rather than orthogonally. The observation that the C–N Anomaly 6B intersects an EPR Anomaly 6B at the southwestern ends of both Hernando Scarp (Fig. 7) and Grijalva Scarp (Fig. 2) confirms that the initial Pacific–Cocos–Nazca triple junction was of the ridge–ridge–ridge type, not the ridge–ridge–transform type to be expected if the plate-splitting fracture followed an east-flank fracture zone to an EPR transform.

4. Evidence from south of Panama

East–west magnetic lineations south of the Azuero Peninsula (Fig. 9) were identified by Lonsdale and Klitgord (1978) as a northward-aging Anomaly 6A–6C sequence. This identification implied that north–south C–N spreading had begun as early as 24 Ma, 1

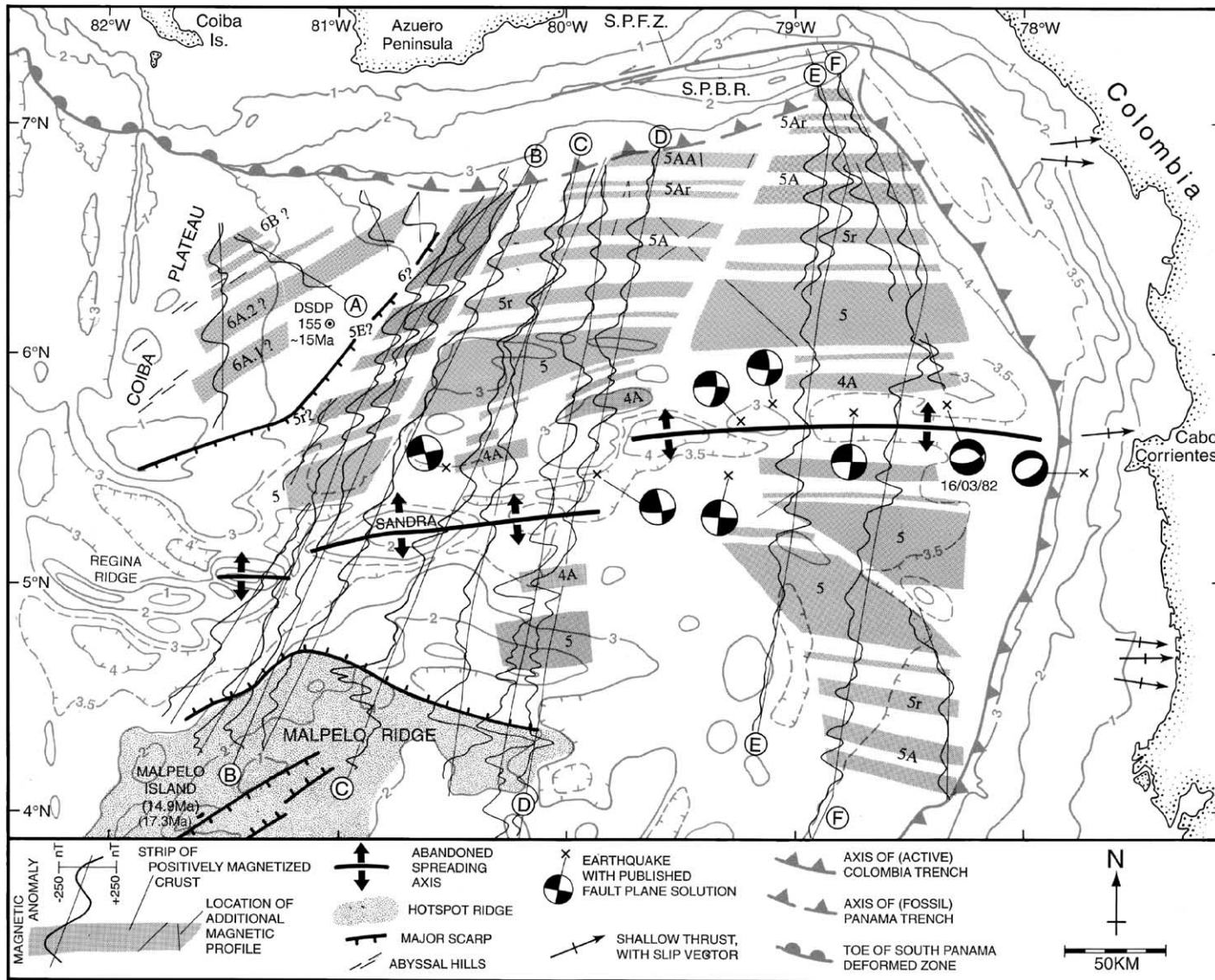


Fig. 9. A new interpretation of magnetic anomalies south of Panama, a region where pre-23 Ma Cocos–Nazca spreading had previously been reported (Lonsdale and Klitgord, 1978). Slip vectors for interplate thrust earthquakes, and “beach-ball” representations of compressional and extensional sectors, are from the Harvard University archive of centroid–moment tensor solutions.

m.y. before any trace of spreading along surviving parts of Grijalva Scarp and a full 4 m.y. before it changed to a north–south direction there. A recent reinterpretation of magnetic profiles in this region near 80°W (Barckhausen et al., 2001) ascribes the anomalies to the Chron 6B–6A sequence of initial C–N spreading though (i) they have a different strike from C–N anomalies of this age elsewhere on either the Cocos or Nazca plates (e.g., Figs. 2 and 8), and (ii) the oceanic basement on the north side of the anomaly identified as 6B is notably smooth (e.g., Lowrie, 1978; profiles C, D of Fig. 10), lacking any evidence of a rifting site that would be conjugate to the roughest, northeastern part of the Grijalva rifted margin. My revised analysis of a larger number of magnetic profiles across the northeastern Panama Basin (Fig. 9) attributes these north-flank C–N anomalies near 80°W, and further east, to the much younger Chron 5A–5 sequence. An excellent match to synthetic (modeled) anomalies, with accretion rates and azimuths consistent with those elsewhere on the C–N flanks, indicates that oceanic crust in the failed trench along the continental margin of the Gulf of Panama (e.g., on profiles C–F of Figs. 9 and 10) is no older than 13.5 Ma. This downward revision of crustal ages means that the seafloor in the northeastern corner of the Panama Basin contains no direct evidence of the timing and pattern of the Early Miocene initiation of C–N spreading. Older C–N crust which might have clarified the early history has been lost by subduction at the now-inactive Panama Trench. Seismic profiles across this turbidite-filled trench (Lowrie, 1978, Westbrook et al., 1995) indicate that the oceanic crust has underthrust the South Panama Boundary Ridge, which is revealed as a sliver of isthmian basement transported east from the slope of the Azuero Peninsula (Fig. 9) by left-lateral Nazca–Caribbean shearing, rather than a conjugate of the initial-rifting ridge along Grijalva Scarp as Lonsdale and Klitgord (1978) had suggested.

Another implication of the younger-than-supposed age of the surviving crust south of the Panama Trench is that the Middle and Late Miocene history of a large part of the C–N plate boundary needs rewriting. A complete rewrite of the history of the eastern Panama Basin would be beyond the scope of this paper, and premature because of continuing data gaps. I sketch and justify a revision of the interpretations of Lons-

dale and Klitgord (1978) and Hardy (1991) only because it helps identify the most likely sites of the oldest C–N crust, and affects speculations on the initial geometry of the Farallon split and the possible role of the Galapagos hotspot plume.

The most important revision concerns the location and function of the (abandoned) spreading center that accreted the crust immediately south of the Panama Trench. The northward aging of this crust is evidence for initial accretion to the Cocos plate, though the plate-defining seismicity study of Molnar and Sykes (1989) seemed to establish that it is now part of the Nazca plate. Lonsdale and Klitgord (1978) thought this crust had spread north from a C–N axis they called Malpelo Rift, which became inactive, transferring its north flank to the Nazca plate, shortly after Chron 5 (i.e., ~9 Ma), leaving abandoned spreading axes 600–700 km south of the Panamanian margin, between Malpelo and Carnegie Ridges (Fig. 10). My magnetic reinterpretation (Figs. 9 and 10) instead shows the crust of the northeastern Panama Basin to be the captured north flank of a spreading center that lies just 150 km south of the margin and continued spreading until about 8.5 Ma (though with the existing rather widely spaced magnetic profiles there is some uncertainty about the pattern and even the identification of anomalies younger than Chron 5). The risecrest intersects the Colombia Trench off Cabo Corrientes, where the axis of that trench changes from a northeasterly to a northwesterly strike. This interpretation relies especially on the bilateral symmetry of magnetic anomalies on profile F (Fig. 10); further west, high volcanic relief near the northeastern end of Malpelo Ridge obscures any lineated magnetic anomalies on the south flank. Bathymetric and seismic profiles support the magnetic identification of a fossil spreading center. Its eastern part (e.g., profiles E and F, Fig. 10) has the axial rift valley typical of many abandoned risecrests (Batiza, 1989); the western part has a high volcanic ridge (Sandra Ridge, profile A of Fig. 10), a common alternative landform (e.g., Lonsdale, 1991). The “abandoned” risecrest is still marked by a band of seismicity, with several recent earthquakes large enough to yield centroid moment tensor (CMT) fault plane solutions (i.e., $m_b > 5.3$). The association of seismicity with an east–west band of rough topography has prompted the suggestion that this is a nascent spreading center, called Sandra Rift by de

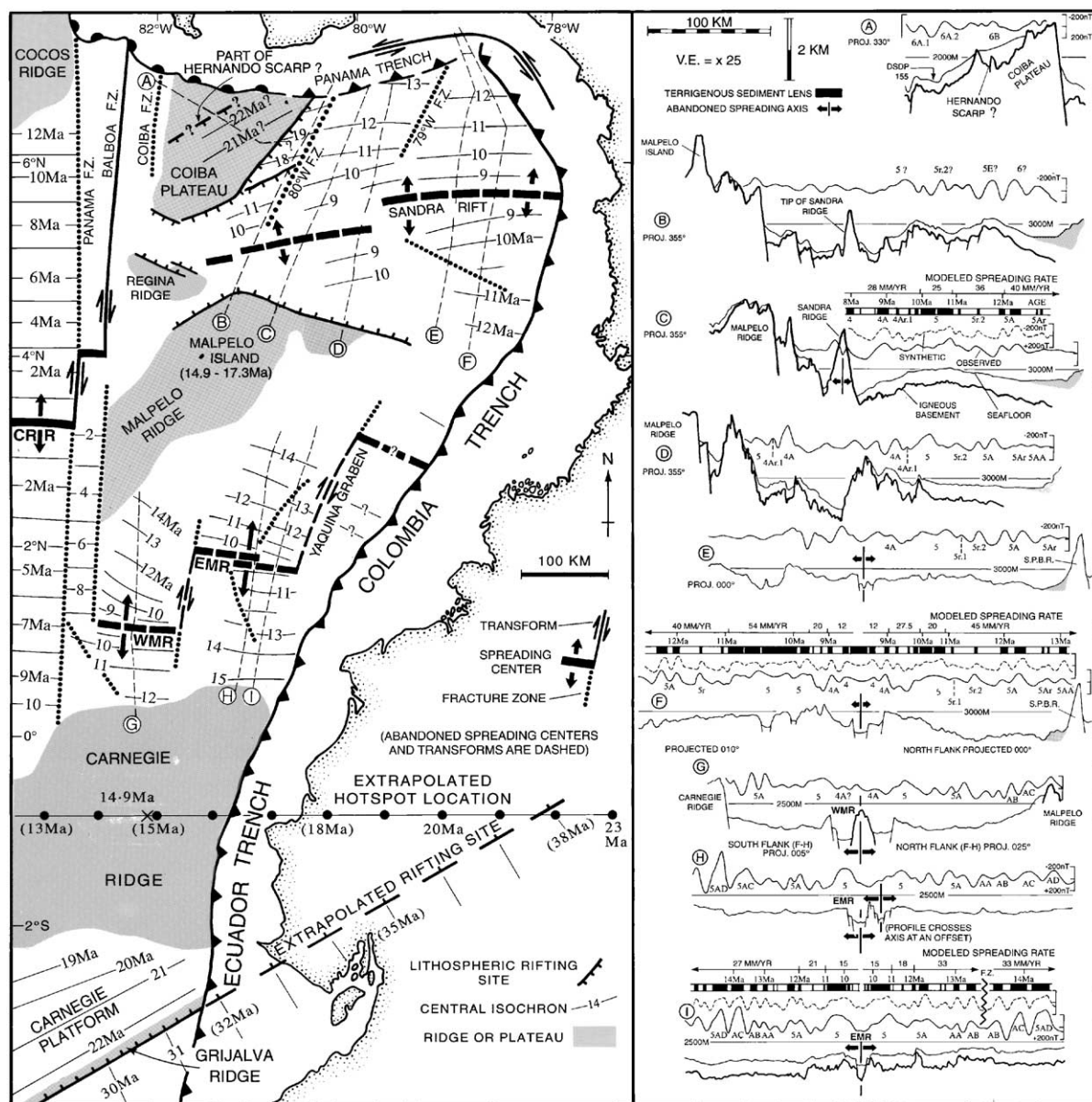


Fig. 10. Revised interpretation of the pattern of crustal isochrons and abandoned plate boundaries in the eastern Panama basin. Profiles B–F are among those plotted in Fig. 9. The 14.9 Ma radiometric date of Malpelo Island lavas is used to help extrapolate the Galapagos hotspot location to its intersection with the Grijalva Rift; if the 17.3 Ma date of Hoernle et al. (2002) is evidence that the hotspot axis was centered near Malpelo Island at that time, the “extrapolated 23 Ma hotspot location” would be even closer to the extrapolated Grijalva rifting site.

Boer et al. (1988), beginning to detach a “North Nazca” microplate from the Nazca Plate. In light of the magnetic evidence, I interpret the modern seismicity along Sandra Rift as evidence of residual or reactivated tectonism along an imperfect Late Miocene

plate suture. Some of the earthquakes, notably the 16/03/82 event (Fig. 9) have a normal-faulting focal mechanism appropriate for a rifted “not-quite-abandoned” spreading axis, but most of the CMT solutions indicate strike-slip mechanisms. Better de-

termination of earthquake locations, and higher resolution swath mapping of the Sandra Rift structure, would be needed to establish whether these were (1) right-lateral events along (almost) abandoned transform faults linking the offset spreading axes, as interpreted by Bergman and Solomon (1984) and de Boer et al. (1988), or (2) the results of left-lateral slip along the formerly accreting plate boundary, sharing the Nazca–Caribbean shear with the left-lateral Southern Panama Fault Zone at the isthmian margin. I favor the second alternative, because offsets of the spreading axis seem too short to produce large earthquakes, even in fairly old lithosphere.

How far west does Sandra Rift and the young (<13.5 Ma) crust of its northern flank extend? The unambiguously identified anomaly 5-5A sequence can be traced (Fig. 9) from the northern Colombia Trench, across an apparently oblique 30 km-offset fracture zone that intersects the Panamanian margin near 79°W, to another oblique fracture zone that intersects the margin near 80°W. Immediately west of the “80°W” oblique fracture zone is a well traveled 25 km-wide corridor (south of Azuero Peninsula, on the route between the Panama Canal and the intensively studied DSDP Site 504B) where closely spaced profiles show rougher, more rifted, basement relief and a different magnetic pattern that I cannot match with any continuous part of the reversal sequence. My preferred, but still tentative interpretation (Fig. 9) is that the southern part of this narrow “scientific shipping lane” may have 12–10 Ma (Chron 5r-5) crust that accreted at a western extension of Sandra Rift, but the crust in the northern part is significantly older (Chron 6-5E) and must have accreted at a different axis, e.g., at Malpelo Rift. Still further west is the shallow, apparently uplifted, crust of Coiba Plateau, which slopes up to a ~1 km-deep crest at an abrupt western escarpment, and is definitely older than 14 Ma. A minimum age is given by the ~15 Ma paleontologic dating of chalk which directly overlies lava flows at DSDP Site 155, but the unusual composition and interbedded limestone of these flows (Yeats et al., 1973; Van Andel et al., 1973) implies off-axis eruption. Abyssal hills mapped on two Seabeam traverses of the high southwest part of the plateau (Fig. 9) have northeasterly strikes appropriate for Early Miocene C–N crust, but most of the lower slopes of this tilted block have a thick non-conformable sediment cover

that obscures basement relief. The few suitably oriented magnetic profiles indicate high amplitude, northeast-striking anomalies (e.g., those labeled 6A.1? and 6A.2? in Fig. 9), but better data coverage would be needed for unambiguous identification on this small patch of crust.

The northeastern end of Malpelo Ridge, a Cocos-plate trail of the Galapagos hotspot that was captured by the Nazca plate (Johnson and Lowrie, 1972; Hey, 1977), also predates the adjacent Sandra Rift rise-flank. Middle Miocene chalk dated at 13–15 Ma overlies volcanic basement in the central part of this northeastward-aging ridge (Lonsdale and Fornari, 1980), and Fontignie et al. (1993); plus D. Fontignie, pers. comm. 1999) obtained a radiometric (K/Ar) date of 14.9 ± 0.5 Ma for lavas from Malpelo Island; subsequent $\text{Ar}^{40}/\text{Ar}^{39}$ analyses of another set of volcanic samples from the island (Hoernle et al., (2002)) yielded age estimates between 15.8 ± 0.1 Ma and 17.3 ± 0.3 Ma. The crest of Malpelo Ridge near the island has a 20 km-wide rift valley that is parallel to similar troughs on the once-contiguous Cocos Ridge, striking 058° (Lonsdale and Fornari, 1980). Where the ridge abuts the narrow south flank of Sandra Rift (profiles C and D of Fig. 10) another 20 km-wide trough has a divergent 098° strike (Fig. 9).

The simplest interpretation of the structural and crustal-age patterns mapped in Fig. 10 is that Sandra Rift was a C–N spreading axis that propagated westward from at least 12 Ma to about 9 Ma, into older Cocos-plate lithosphere that had accreted at the Malpelo Rift system and its northeast-striking predecessor, and had been partly buried by a hotspot ridge. As it propagated, Sandra Rift overlapped the concurrently spreading eastern segment of Malpelo Rift, where spreading slowed after 12 Ma (profiles H and I, Fig. 10). The intervening crust probably rotated as a short-lived “Malpelo microplate”, though clockwise rotation (e.g., of isochrons on the north flank of Malpelo Rift) was modest, except near the propagating rift tip, where the 40° change in strike of the crestal graben of Malpelo Ridge is ascribed to local tectonic rotation. Part of the eastern boundary of the microplate for at least some of its history was probably Yaquina Graben (Fig. 10) but the tectonic role and history of this major rift valley, which has 3 km of structural relief (van Andel et al., 1971), is uncertain. Structural similarity to the shorter trough that links western and eastern

segments of Malpelo Rift suggests that Yaquina Graben originated as a transtensional C–N transform valley, and satellite altimetry suggests that this deep valley ends, presumably by linking to another extinct C–N spreading segment, in a region near 3.3°N that lacks adequate survey data and is somewhat south of the extinct “Buenaventura Rift” postulated by Hardy (1991). By 9 Ma, with the eastern Malpelo Rift already failing, the western boundary of the microplate stabilized at a new transform fault that cut across the combined Cocos–Malpelo Ridge to link the western Malpelo Rift to the western end of the zone of lithospheric rifting at the tip of the propagating Sandra Rift spreading center. Shortly thereafter this new transform fault system lengthened to intersect the Middle America Trench, and spreading centers throughout the eastern Panama Basin became extinct as the whole region was captured by the Nazca plate.

If this simplest tectonic interpretation is the correct one, Coiba Plateau is the most likely Panama Basin site to have Early Miocene crust containing evidence of initial C–N spreading. It would have accreted before the ~17–15 Ma passage of the Galapagos hotspot past its longitude, and be conjugate to the 23–19 Ma crust of the Carnegie Platform, between Carnegie Ridge and the eastern part of Grijalva Scarp (Fig. 2). The identification of Anomalies 6A and 6B shown in Figs. 9 and 10 (profile A) is, however, too uncertain to validate Lonsdale and Klitgord’s (1978) suggestion that a captured part of Hernando Scarp (which would be adjacent to Anomaly 6B) crosses the plateau and isolates a remnant of the Farallon plate in its northwest corner. Regional geography is consistent with this hypothesis, in that the implied location of the captured part of the scarp is laterally displaced about 600 km south of the extrapolated position of the subducted scarp beneath Costa Rica, a distance equal to the northward separation of the Cocos plate from the Nazca plate (and from Coiba Plateau) since spreading ceased at Sandra and Malpelo Rifts. Panama Basin geography is not consistent with the suggestions of Meschede and Barckhausen (2001) that Coiba Ridge represents the oldest part of Cocos Ridge (i.e., the Cocos Plate trail of the Galapagos hotspot), whereas Malpelo Ridge is the 14–11 Ma product of a different hotspot. As Lonsdale and Klitgord (1978) explained, (i) the amount of C–N strike-slip motion along the Panama transform fault system since the

~8.5 Ma capture of the eastern Panama Basin (including Malpelo Ridge) by the Nazca plate, as recorded by the width of post-8.5 Ma C–N crust accreted at the Costa Rica Rift (Fig. 10), equals the observed separation of Malpelo Ridge (not Coiba Plateau) from Cocos Ridge, and (ii) the pattern of crustal isochrons on the flank of Malpelo Rift fits with Malpelo and eastern Carnegie Ridges being the coeval ~17–13 Ma trails of a Galapagos hotspot centered near the C–N plate boundary, as in the model of Johnson and Lorie (1972). An alternative hypothesis in which Malpelo Ridge, far from being unrelated to Carnegie Ridge as suggested by Meschede and Barckhausen (2001), was split off an ancestral east–west Carnegie Ridge by a subsequent episode of C–N spreading (van Andel et al., 1971; Werner et al., 2003) can be rejected because of the unrifted structure of most of the ridges’ margins, and because it implies that the parallelism of Malpelo Ridge to Cocos plate motion is a mere accident of the rate of (hypothetical) westward propagation of the Malpelo Rift axis.

5. The west flank of the EPR

Crust that accreted to the Pacific flank of the EPR during the 30–20 Ma period provides evidence on three questions relevant to the 23 Ma Farallon split: the pattern of east-flank fracture zones that plate fragmentation may have exploited; the changing spreading directions that occurred where Pacific–Farallon spreading axes changed into Pacific–Cocos ones; and pre-23 Ma plate fragmentation that may have influenced or fostered fission into Cocos and Nazca plates.

Satellite altimetry (Sandwell and Smith, 1997, and www://topex.ucsd.edu) and 4 north–south Seabeam 2000 swaths (Scripps Institution of Oceanography, unpublished data; www://sioexplorer.ucsd.edu) show that at 120°–130°W the generally smooth EPR flank in the 1870 km-long strip between the large-offset Clipperton and Marquesas fracture zones is crossed by three trails of shorter Pacific–Farallon transform faults. Viru fracture zone is just 150 km north of Marquesas fracture zone, and its east-flank trace has already been described (Fig. 2). Two left-stepping offsets (G and N on Fig. 1) at 340 and 780 km south of Clipperton fracture zone have east-flank

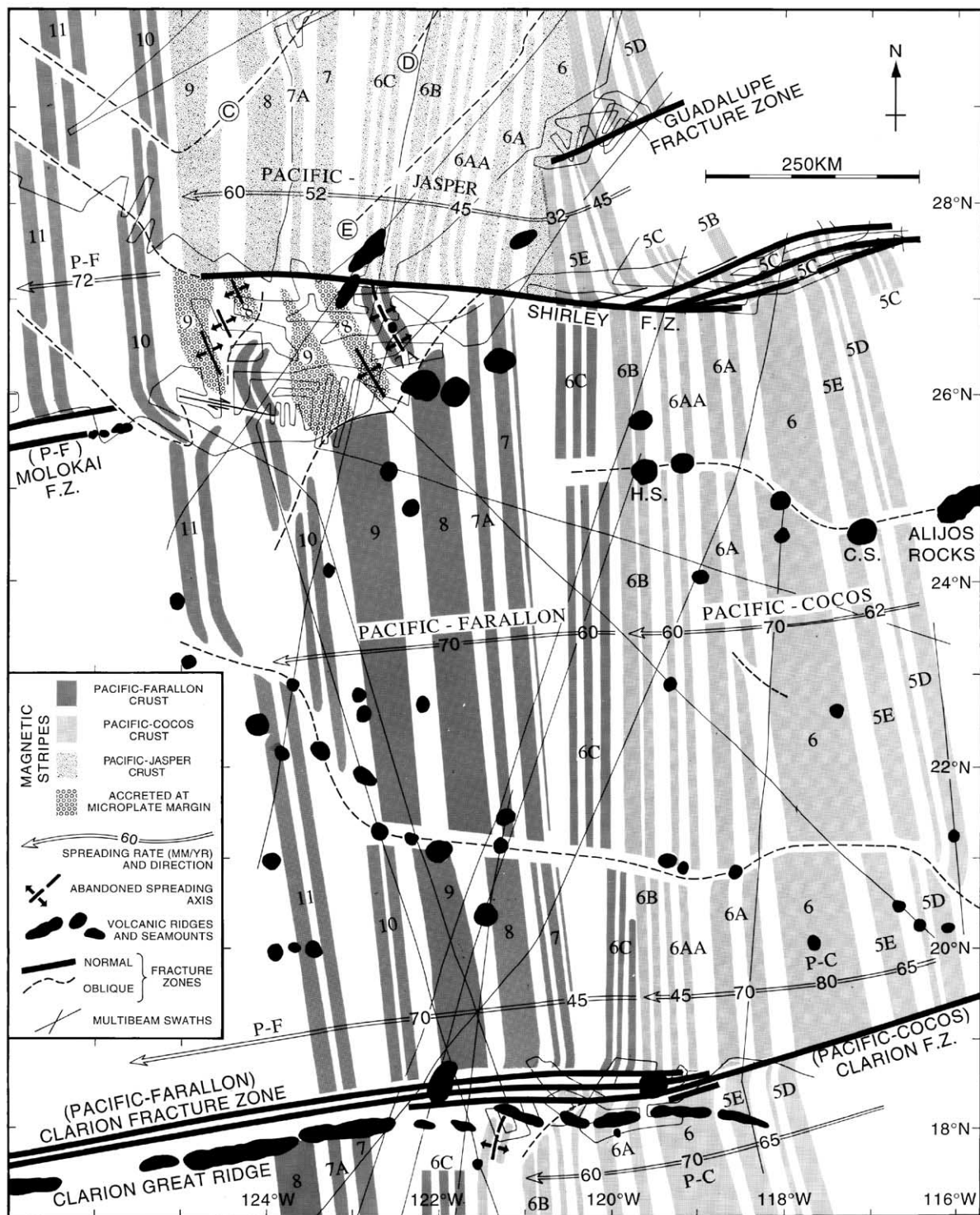
conjugates that intersect the Middle America Trench off Guatemala and off Nicaragua: the Nicaragua fracture zone has a 175 km step of the 23 Ma crustal isochron, 330 km northwest of Hernando Scarp. No trace of the left-stepping Galapagos fracture zone, sometimes suggested as the lineament along which Grijalva Scarp rifted (e.g., Handschumacher, 1976), is seen on altimetry profiles or multibeam swaths east of 130°W; its left offset may have been shifted northward (by propagating rifts) to the Nicaragua and Guatemala transforms during the Oligocene. On older crust further west, Galapagos fracture zone is 900 km south of Clipperton, so any hypothetical eastward extrapolation would bring it some 200 km northwest of the beginning of the Pacific–Cocos–Nazca triple junction on the west flank; its east flank conjugate would be 200 km northwest of Hernando Scarp, where there are no offsets of magnetic stripes (Fig. 7).

The mapped pattern of fracture zones on the west flank of the EPR supports the evidence from geomorphology and magnetics that the Hernando/Grijalva rift did not follow a preexisting EPR fracture zone, at least, not across the young rise flank where lithosphere was less than 8 m.y. old at 23 Ma. There is no unambiguous evidence as to whether the plate-splitting fracture stepped left to the east-flank Galapagos fracture zone on older, since subducted, parts of Farallon plate, but the pattern of crustal isochrons on C–N crust in the eastern Panama Basin (Fig. 10) may be relevant. The 10 Ma isochrons on crust accreted to the Nazca plate at Costa Rica Rift, West Malpelo Rift and East Malpelo Rift describe a staircase of east–west segments that stepped left at 100 km-long transforms, giving an overall trend parallel to the northeast-striking Grijalva rift where spreading originated. The same isochron south of the eastern Sandra Rift lies 200 km north of this overall trend. Perhaps this spreading segment, and others further east (and since subducted) originated at a plate-splitting fracture that was offset ~200 km north of the east end of Grijalva rift, e.g., at the east-flank Galapagos fracture

zone. Alternative explanations are possible, however: the subducted eastern end of Sandra Rift may have been part of the same regularly stepping staircase when east–west C–N spreading segments developed at 19–18 Ma (Fig. 2), with the apparently excessive northward displacement of its surviving, albeit inactive, western part resulting from rapid westward propagation that overlapped intervening (subducted) steps in the staircase, just as the East Malpelo Rift was eventually overlapped.

On the southern EPR the transition from Pacific–Farallon to Pacific–Nazca motion was accompanied by a 25° clockwise change in spreading direction. Judging from the azimuths of magnetic stripes, assumed to have accreted normal to the spreading direction at an orthogonally spreading EPR crest, this rotation was not completed until the acceleration of C–N divergence at 21–22 Ma. As previously noted, it began well before slow C–N spreading was initiated at 23 Ma; where the change in rise-crest azimuth is best constrained (Fig. 2B) it was most rapid during Chron 6Cr (24.7–24.1 Ma), when 8–10° of clockwise rotation are recorded. For a comparable record of the transition from Pacific–Farallon to Pacific–Cocos motion it is necessary to examine the west flank of the EPR, because so little pre-24 Ma east-flank lithosphere has avoided subduction (Figs. 1 and 7), and for the most sensitive record it is best to look as close as possible to the Pacific–Farallon and Pacific–Cocos Euler poles. The northernmost part of the Pacific–Farallon rise-crest at 25 Ma was a long segment north of Clarion transform. It accreted a western rise-flank that is now at 19–27°N, in a thinly sedimented region crossed by many magnetic profiles (e.g., Atwater and Severinghaus, 1989) and several multibeam swaths that define the strike of abyssal hill lineations (Fig. 11). The magnetic interpretation of this region indicates an abrupt 6–8° clockwise rotation during Chron 6Cr. On the spreading axis this rotation was accommodated by initiating or lengthening the short left-stepping nontransform offsets responsible for the “oblique fracture zones” of Fig. 11. The clock-

Fig. 11. Pattern of magnetic stripes in a region of 30–17 Ma crust on the west flank of the EPR (located in Fig. 1) with dense magnetic coverage (e.g., Atwater and Severinghaus, 1989). Abyssal hill lineations along the plotted tracks of multibeam swaths helped constrain the local azimuths of magnetic stripes. Note (i) the evidence for detachment from the Farallon plate of the eastern EPR flank north of Molokai fracture zone during Chron 9 (~28 Ma), and (ii) a change of strike of the Pacific–Farallon axis to an almost north–south “Pacific–Nazca like” azimuth prior to Chron 6Cn (i.e., ~24.5 Ma), gradually reverting to a more northwesterly strike as it becomes a Pacific–Cocos axis during Chron 6B.



wise change in spreading direction opened Clarion transform into a broader structure with strike-slip fault zones that reoriented to an east–west strike, and were linked by short intra-transform spreading axes that accreted crust with north–south abyssal hills (Fig. 12). During Chron 6B, as C–N spreading was starting, the spreading axes rotated in the opposite, counter-clockwise direction. This eliminated the left-stepping offsets, converting them (after a brief “zero-offset” phase) to right-stepping offsets as counter-clockwise rotation continued through Chron 6A. By then, the Pacific–Cocos axis had backed to a more northeasterly strike than the pre-25 Ma Pacific–Farallon axis, and by ~19 Ma in Chron 6 the counter-clockwise rotation had closed Clarion transform to a single strike-slip fault zone. Its west flank trace is a fracture zone (Fig. 11) which strikes 074° , compared to 082° for the multi-stranded pre-25 Ma Pacific–Farallon fracture zone. Satellite altimetry of Clipperton fracture zone at 121 – 123° W (Sandwell and Smith, 1997) indicates that the long Clipperton transform also existed briefly as a broad, segmented east–west structure, immediately before the change from Pacific–Farallon to Pacific–Cocos motion gave it a more northeasterly strike than it had ever had before.

The simplest interpretation of the rise-flank structural lineations that record the relative motion of the Pacific plate with respect to the Farallon plate and its Cocos and Nazca daughters is that 1–2 m.y. before the daughters began to spread apart the entire northeast-moving Farallon plate changed direction to a more easterly (Nazca-like) course. After the Farallon plate split, its northern (Cocos) half changed course back toward the northeast. Determining from evidence on the west flank of the EPR whether there was small differential movement between the nascent Cocos and Nazca plates before they began to spread apart would require more extensive high-resolution surveys to test, for example, whether the clockwise rotation of EPR spreading between Chrons 7 and 6B was generally greater in the south than in the north.

The magnetic anomaly interpretation of Fig. 11 also shows that during Chron 9 (28–27 Ma) a large slab of Farallon lithosphere north of Shirley fracture zone (now near 27° N) broke away as an independently moving plate. This small plate here called the Jasper plate, extended 750 km north to Murray fracture zone; spreading on the west flank of its western

(EPR) margin was responsible for a band of ~27.5–19.5 Ma crust with NNE-striking magnetic anomalies, centered near Jasper Seamount at 30.5° N, 123° W (Lonsdale, 1991). The principal evidence for the independent existence of this plate is that the history of spreading center reorientation recorded by the “Pacific–Jasper” Anomaly 9 to Anomaly 6 sequence (shown in part in Fig. 11) is quite different from that already described to the south. From Chron 9 to Chron 6AA there was a steady 12° clockwise rotation as spreading slowed, and if the magnetic stripes lie along meridians to a moving Euler pole, it was a different one than the poles that describe Pacific–Farallon and Pacific–Cocos motions during the same time interval. The clockwise rotation of Pacific–Jasper spreading direction led to the development of a staircase of left-stepping nontransform offsets, all of which migrated northwards, leaving the oblique fracture zones A–E of Lonsdale (1991). Tectonic complications apparent from Fig. 11, but irrelevant to the story of Farallon fission and therefore to be discussed elsewhere (revising the tectonic history of Lonsdale, 1991), are (i) the temporary presence 27–26 Ma of a microplate at the Pacific–Jasper–Farallon RFF triple junction, and (ii) apparent incorporation of the Jasper plate into the Cocos plate at 19.5 Ma, causing the EPR crest north of Shirley transform to rapidly reorient and reorganize (e.g., by development of new offsets such as Guadalupe transform), in a manner reminiscent of the concurrent reorganization of the C–N rise crest.

This loss from the Farallon plate of ~800 km of subducting margin occurred soon after the ~28.5 Ma (middle of Chron 10) detachment of a slab of Farallon lithosphere that had been entering another 625 km length of the California subduction zone between Murray and Pioneer fracture zones; it became the Monterey plate (Lonsdale, 1991). The principal cause of detachment of Jasper and Monterey plates may have been the increasing resistance to subduction of northern parts of the Farallon plate, where the lithosphere entering the California Trench was becoming increasingly younger as the continental margin approached the EPR crest. The loss of more than 1400 km of subducting margin between 28.5 and 27.5 Ma should have changed the driving forces propelling the Farallon plate, affecting its motion and perhaps, as discussed below, its integrity.

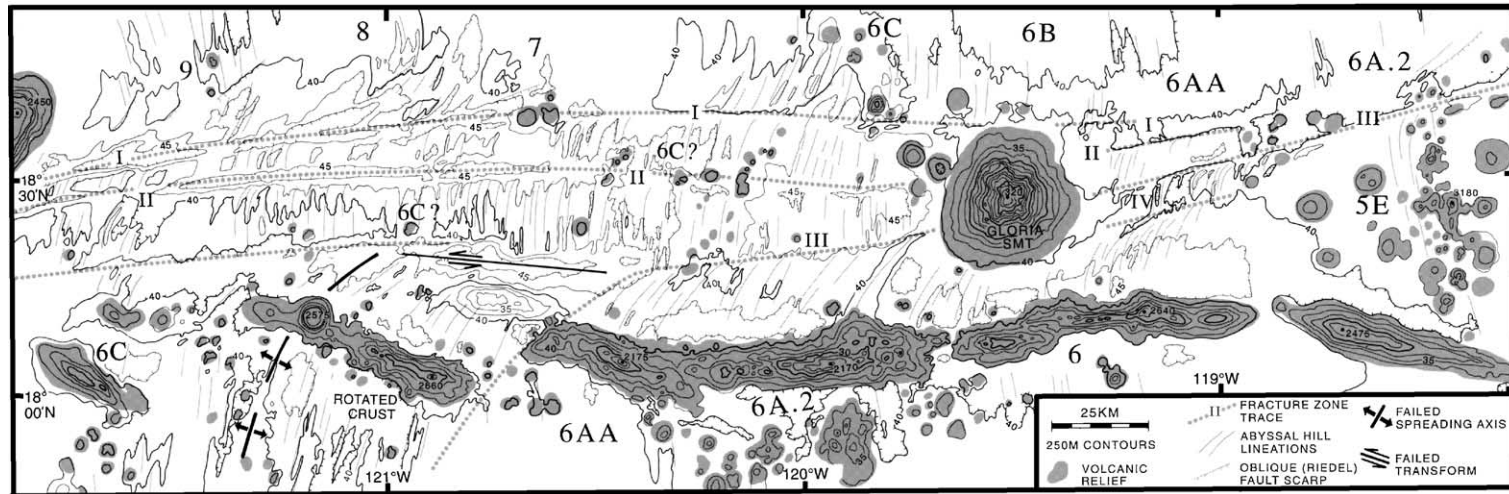


Fig. 12. Structural interpretation of a multibeam sonar survey of the short length of Clarion fracture zone formed during the brief period of east–west spreading at 24.5–23 Ma; a more detailed view of part of the fracture zone mapped in Fig. 11. The centers of magnetic stripes (see Fig. 11) are labeled (9, 8, 7 etc); locations of stripe 6C are poorly constrained on the narrow strips of crust between traces “I”, “II”, and “III” of this multi-stranded fracture zone. The “failed transform” along trace III and the intersecting “failed spreading center” were parts of the Pacific–Cocos boundary abandoned when a northward-migrating left-stepping offset intersected the right-stepping Clarion transform during Chron 6AA (see Fig. 11).

6. Discussion: why did the Farallon plate fission?

The analytic modeling of Wortel and Cloetingh (1981) supported the suggestion of Lonsdale and Klitgord (1978), that the source of the extensional stress that tore the Farallon plate apart was the divergent pull of lithosphere slabs falling down the Middle American and South American subduction zones. Further support comes from the resemblance in structure and pattern of the fissural Alvarado and Sarmiento Ridges to the linear volcanic ridges recently built on young Pacific flanks of the EPR (e.g., Cormier et al., 1997; Scheirer et al., 1998), for the former are assumed to be products of the plate-splitting episode and the latter (located in Fig. 1) have been attributed to divergent slab pull acting on a fast-moving oceanic plate (Sandwell et al., 1995). A necessary caution is that the ridges off northern Peru have not been radiometrically dated, and the assumption that they record diffuse extension of the Farallon plate prior to its 23 Ma split rests on their restriction to lithosphere older than 25 Ma (Fig. 2), i.e., to lithosphere strong enough to transmit far-field tensile stress before 23 Ma. Sandwell et al. (1995) explain that their diffuse extension model predicts that, in the absence of other significant plate driving forces such as ridge push, the axis of maximum tensile stress is parallel to the absolute motion of the plate. The 050–055° strike of Alvarado and Sarmiento Ridges is significantly oblique to the pre-25 Ma absolute motion of the Farallon plate, recorded by the 040° strike of Nazca Ridge (Fig. 1), but may be parallel to its motion during its final phase as an intact plate, following the 25–24 Ma change in direction that rotated Pacific–Farallon spreading 6–10° clockwise.

Divergence of the slab pull from the Middle American and South American subduction zones had been a feature of the Farallon plate stress field throughout the Paleogene. Why was it at the beginning of the Miocene that fission occurred? Handschumacher (1976) and Lonsdale and Klitgord (1978) favored a hypothesis involving change in Farallon plate geometry and driving forces after its northern parts had been completely subducted during collision of the EPR axis with the North American margin. An updated version that uses new information on the final stages of EPR spreading off North America is that the slab-pull stress from the Californian subduction zone, which extended

to the southern tip of Baja California, was eliminated from the Farallon plate at 28.5–27.5 Ma when large slabs of the plate north of Molokai fracture zone were detached, as discussed above; at the time this fracture zone intersected the convergent margin at the south end of the Californian Trench (Fig. 13), according to the Pacific–North America plate reconstructions of Atwater and Stock (1998). Once the slab pull normal to the 325°-striking California subduction zone no longer acted on the Farallon plate, the northern half of the reduced plate was pulled more to the north by the slab in the more westerly striking Middle American subduction zone, and this suddenly increased divergence from the South American pull may have been enough to stretch and (within a few million years) fission the equatorial region of the plate. Another factor that would have gradually increased the divergent northward pull from the Middle American subduction zone was the steadily changing geography of that zone as the North American plate moved west past the Caribbean plate. In the plate reconstructions of Ross and Scotese (1988), between 44 and 23 Ma this motion lengthened the subduction zone between Baja California and central Panama by 10%, and changed its strike from 313° to 302°.

If fission of the Farallon plate occurred at the beginning of the Miocene because extensional stress from the convergent plate boundaries had increased above some plate-splitting threshold, that threshold may have been reduced by weakening of equatorial parts of the plate by the Galapagos plume. Hey (1977) suggested that the plate broke apart when the hotspot was born, or when it intersected a pre-existing line of weakness such as an EPR fracture zone. There is good evidence that the Galapagos hotspot was born well before the early Miocene. Though there are no dates for its obvious volcanic trails older than the 17.3 Ma date of Malpelo Island, the Cretaceous Caribbean large igneous province has been interpreted as the result of arrival of its plume head at the surface (e.g., Duncan and Hargraves, 1984; Sen et al., 1988). The estimated site of the hotspot when the plate split (Figs. 9 and 13) was on since-subducted ~15 m.y.-old lithosphere, near the (extrapolated) location of the Hernando/Grijalva rift, and near the western end of the east-flank Galapagos fracture zone. It was also presumably at the southwest end of a hotspot ridge, striking 040° (parallel to the coeval Nazca

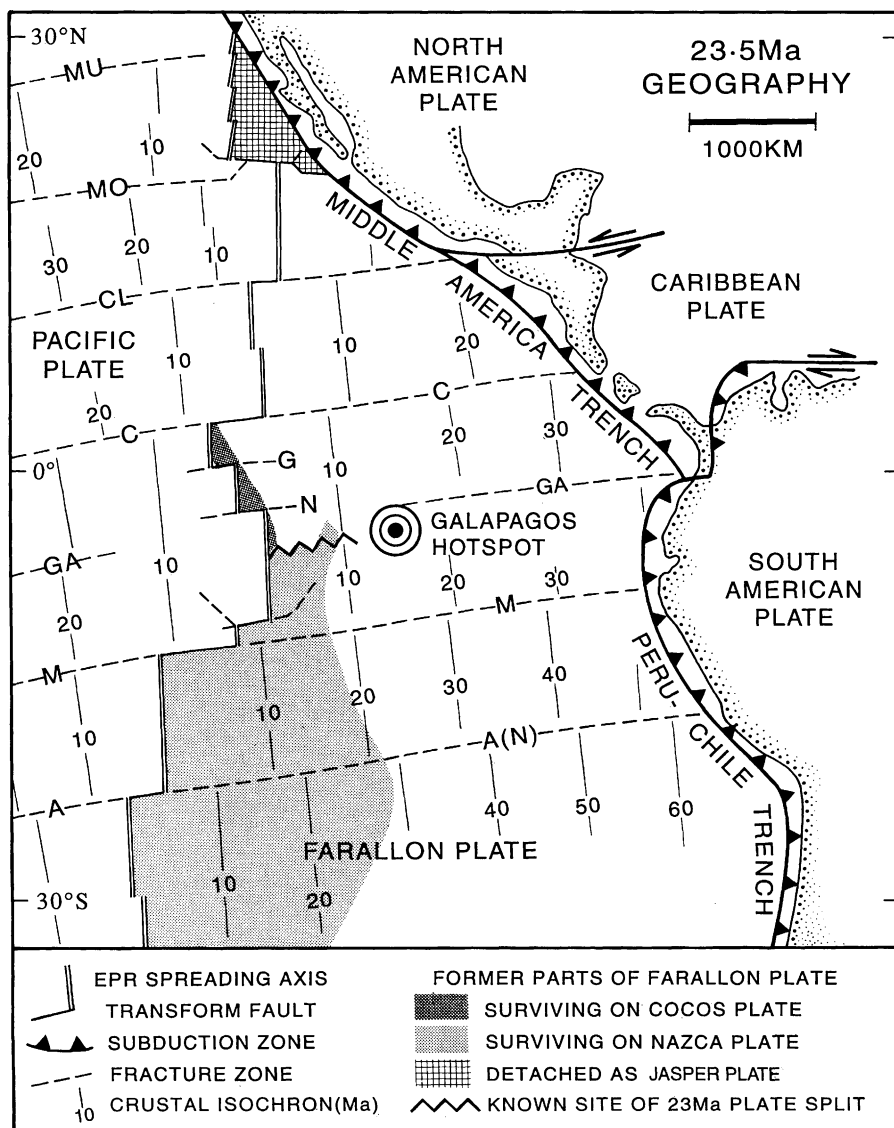


Fig. 13. Reconstruction of the geography of the Farallon plate just before its split into the Cocos and Nazca plates. Note that most of the plate has subsequently been lost by subduction.

Ridge) across the Farallon plate to the Caribbean margin. Plate stretching was apparently able to break new fractures through young normal lithosphere between the hotspot and the risecrest (e.g., the Hernando/Grijalva rift), but pre-existing lines of weakness, either the hotspot trail (with thick weak crust and reheated mantle) or the fracture zone, may have been a prerequisite for rupturing the much older lithosphere between the hotspot and the trench. Unless lithosphere

up to 35 m.y. old (Fig. 13) had ruptured the plate would not have been completely split, and intra-Farallon rifting would have been arrested at a stage similar to the diffuse extension zones on the west flank of the EPR, developing fissural volcanism but no spreading center.

Whether or not existence of the Galapagos hotspot was a prerequisite for this oceanic plate fission, a likely effect of its presence was to make long seg-

ments of the resulting rifted margins the oceanic equivalents of volcanic rifted margins, the lava-rich variety of continental margin that develops where continental lithosphere ruptures over atypically hot asthenosphere (White and McKenzie, 1989). Assessing the regional thermal influence, or direct magma-supplying role, of the Galapagos hotspot on construction of the high Grijalva, Alvarado and Sarmiento Ridges (500–1000 km from the estimated position of the axis of the hotspot plume at 23 Ma) may be possible by analyses of these ridges' lavas.

7. Conclusions: where, how and when the Farallon plate split apart

The Farallon plate fissioned into Cocos and Nazca halves at a 3000 km-long rupture zone that extended from the EPR crest to the vicinity of the junction between Middle American and South American subduction zones, breaking through oceanic lithosphere of the east flank of the EPR that was as much as 30–40 Myr old. The rupture zone evolved into a conjugate pair of rifted oceanic margins, analogous to the rifted continental margins left by rupture of continental lithosphere, then into the C–N spreading center. Subduction has removed all but 680 km of the southern (Grijalva) rifted margin; all that remains is its southwest end where lithosphere less than 8.5 Myr old was ruptured. Even less of the northern (Hernando) conjugate margin survives: just 75 km of its southwestern end off the Nicoya peninsula, mostly on the outer slope of the Middle America Trench, and perhaps an equal length on the uplifted Coiba Plateau south of Panama. Structural and magnetic patterns alongside the surviving parts of the rift show that where the rupture zone crossed the young (<8 Myr-old) EPR flank it was typical rise-flank crust that rifted apart, in a direction probably orthogonal to absolute motion of the Farallon plate. Extant parts of the rift have small en echelon left steps, and there is inconclusive evidence from the pattern of C–N spreading axes in the easternmost Panama Basin that in older, since subducted, lithosphere there was a larger left step, possibly to a preexisting line of weakness such as the east-flank Galapagos fracture zone or the Galapagos hotspot trail.

Splitting of young (<2 Myr-old) lithosphere on the near-axis rise-flank resulted in a few hundred meters of uplift at narrow (5–10 km-wide) rift shoulders alongside discontinuous inward-facing fault scarps. Rifting may have produced a larger scale of tectonic relief where it affected older and therefore thicker oceanic lithosphere, but the structure of the surviving rifted margin west of Ecuador is difficult to interpret: where mature 2–7.5 Myr-old rise-flank was rifted, much of the tectonic relief has been obscured by ridge-building fissural volcanism, and where the rifting site approaches the subduction zone some of its prominent faulted topography may be attributable to recent trench–slope tectonism rather than to Miocene plate-splitting.

The narrowly defined rifted margins were embedded in a wider zone of stretched and fractured lithosphere, known to extend 250 km from the plate-splitting site on the better preserved southern side. Fractures here are subparallel to the rifted margins, and some of them are occupied by 1–2 km-high volcanic ridges. This broad zone of diffuse extension and fissure eruption is mainly on pre-25 Ma lithosphere, with some non-eruptive fractures extending to the 24 Ma crustal isochron; it is inferred to have become extinct once rifting became localized at a site of complete lithospheric rupture, and Farallon plate stretching was replaced by C–N spreading. This spreading was initially slow and perhaps oblique, at an axis along the feet of the rifted-margin fault scarps, but accelerated and changed to a north–south direction (parallel to the divergence of the sibling plates) after 2–3 Myr. The change in strike of C–N spreading axes was accompanied by rise-crest segmentation and propagation, with some overlapped segments being abandoned on the south flank. A much later episode of rift propagation led to abandonment of other C–N axes in the eastern Panama Basin.

Timing of the initiation of C–N spreading is well constrained by the presence of magnetic anomalies from Chron 6B (23.0–22.6 Ma) at the youngest C–N crust along the rifted oceanic margins. Previous interpretations of earlier Chron 6CC–N spreading and of north–south Chron 6AA–6B spreading were derived from misidentification of magnetic anomalies in the northeastern Panama Basin. Inter-plate spreading was the culmination of a process of plate stretching and rifting that probably became intense after ~24.5 Ma,

when the motion of the Farallon plate changed in a way that made it significantly more oblique to the Middle American slab pull.

Acknowledgements

I thank the Governments of Costa Rica, Panama, Colombia, Ecuador and Peru for permission to collect marine geophysical data within their exclusive economic zones, and the crews and scientific parties of several R/V Melville and R/V Revelle expeditions. Special thanks to Dr. D. Chadwell for diverting his cruise leg to acquire an EM-120 sonar swath across the ridges off northern Peru, and to Dr. J. Stock for a helpful review. The research was partly funded by NSF grants OCE 93-14679 and OCE 94-00707.

References

- Atwater, T., 1989. Plate tectonic history of the northeast Pacific and western North America. *Geology of North America, DNAG,N*, pp. 21–72.
- Atwater, T., Severinghaus, J., 1989. Tectonic maps of the northeast Pacific. *Geology of North America, DNAG,N*, pp. 15–20.
- Atwater, T., Stock, J., 1998. Pacific–North America plate tectonics of the Neogene southwestern United States: an update. *Int. Geol. Rev.* 40, 375–402.
- Barckhausen, U., Ranero, C.R., von Huene, R., Cande, S.C., Roesser, H.A., 2001. Revised tectonic boundaries in the Cocos Plate off Costa Rica: implications for the segmentation of the convergent margin and for plate tectonic models. *J. Geophys. Res.* 106, 19207–19220.
- Batiza, R., 1989. Failed rifts. *Geology of North America, DNAG,N*, pp. 177–186.
- Bergman, E.A., Solomon, S.C., 1984. Source mechanisms of the earthquakes near mid-ocean ridges from body wave inversion: implications for the early evolution of oceanic lithosphere. *J. Geophys. Res.* 89, 11415–11441.
- Bourasseau, I., Juteau, T., Karpoff, A.M., Bougois, J., Bellon, H., 1993. Exploration des structures volcaniques de la ride d'accrétion de Mendana au large du Pérou: résultats de la campagne Nautipere du submersible NAUTILE, Avril 1991. *C.R. Acad. Sci.* 317, 1097–1103.
- Cande, S.C., Kent, D.V., 1995. Revised calibration of the geomagnetic polarity timescale for the late cretaceous and cenozoic. *J. Geophys. Res.* 100, 6093–6095.
- Cormier, M., et al., 1997. Sojourn leg 1: detailed study of the asymmetries about the East Pacific Rise 15°30'–20°S Ridge Events, vol. 8, pp. 1–5.
- de Boer, J.Z., Defant, M.J., Stewart, R.H., Restrepo, J.F., Clark, L.F., Ramirez, A.H., 1988. Quaternary calc-alkaline volcanism in western Panama: regional variation and implication for the plate tectonic framework. *J. South Am. Earth Sci.* 1, 275–293.
- Duncan, R.A., Hargraves, R.B., 1984. Plate tectonics evolution of the Caribbean region in the mantle reference frame. *Geol. Soc. Am. Mem.* 16, 81–93.
- Fontignie, D., Schilling, J.G., Kingsley, R., Delaloye, M., 1993. L'origine de l'Isle de Malpelo (Est-Pacifique) dans le contexte du point chaud "Galapagos", (abstract). *Reunion Soc. Suisse de Mineral. Pet.*
- Goff, J.A., Cochran, J.R., 1996. The Bauer Scarp ridge jump: a complex tectonic sequence revealed in satellite altimetry. *Earth Planet. Sci. Lett.* 141, 21–33.
- Gutscher, M.A., Malavieille, J., Lallemand, S., Collot, J., 1999. Tectonic segmentation of the North Andean margin: impact of the Carnegie Ridge collision. *Earth Planet. Sci. Lett.* 168, 255–270.
- Handschumacher, D.W., 1976. Post-Eocene plate tectonics of the eastern Pacific. *Am. Geophys. Union Geophys. Mono.* 19, 177–202.
- Hardy, N., 1991. Tectonic evolution of the easternmost Panama Basin. *J. South Am. Earth Sci.* 4, 261–270.
- Hekinian, R., Bideau, D., Cannat, M., Francheteau, J., Hebert, R., 1992. Volcanic activity and crust–mantle exposure in the ultra-fast Garrett transform fault near 13deg28min5 in the Pacific. *Earth Planet. Sci. Lett.* 108, 259–275.
- Hey, R., 1977. Tectonic evolution off the Cocos–Nazca spreading center. *Geol. Soc. Amer. Bull.* 88, 1404–1420.
- Hoernle, K., van den Bogaard, P., Werner, R., Lissinna, B., Hauff, F., Alvarado, G., Garbe-Schonberg, D., 2002. Missing history (16–71 Ma) of the Galapagos hotspot: implication for the tectonic and biological evolution of the Americas. *Geology* 30, 795–798.
- Huchon, P., Bourgois, J., 1990. Subduction-induced fragmentation of the Nazca Plate off Peru: Mendana fracture zone and Trujillo Trough revisited. *J. Geophys. Res.* 95, 8419–8436.
- Johnson, G.L., Lowrie, A., 1972. Cocos and Carnegie ridges—result of the Galapagos "Hot Spot"? *Earth Planet. Sci. Lett.* 14, 279–280.
- Kimura, G., Silver, E.A., Blum, P., et al., 1997. Site 1039. *Proc. ODP Initial. Rep.* 170, 45–93.
- Lonsdale, P., 1988. Structural pattern of the Galapagos microplate and evolution of the Galapagos triple junctions. *J. Geophys. Res.* 93, 13551–13574.
- Lonsdale, P., 1989. Segmentation of the Pacific–Nazca spreading center 1°N–20°S. *J. Geophys. Res.* 94, 12197–12225.
- Lonsdale, P., 1991. Structural patterns of the Pacific floor offshore of peninsular California. *AAPG Mem.* 47, 87–125.
- Lonsdale, P., 1994. Structural geomorphology of the Eltanin fault system and adjacent transform faults of the Pacific–Antarctic boundary. *Mar. Geophys. Res.* 16, 105–143.
- Lonsdale, P., 1995. Segmentation and disruption of the East Pacific Rise in the mouth of the Gulf of California. *Mar. Geophys. Res.* 17, 323–359.
- Lonsdale, P., Fornari, D., 1980. Submarine geology of Malpelo Ridge, Panama Basin. *Mar. Geol.* 36, 65–83.
- Lonsdale, P., Klitgord, K.D., 1978. Structure and tectonic history of the eastern Panama Basin. *Bull. Geol. Soc. Am.* 89, 981–999.

- Lowrie, A., 1978. Buried trench south of the Gulf of Panama. *Geology* 5, 434–436.
- Mammerickx, J., Klitgord, K.D., 1982. Northern East Pacific Rise: evolution from 25 m.y.B.P. to the present. *J. Geophys. Res.* 87, 6751–6760.
- Mammerickx, J., Anderson, R.N., Menard, H.W., Smith, S.M., 1975. Morphology and tectonic evolution of the east-central Pacific. *Geol. Soc. Amer. Bull.* 86, 111–118.
- Massell, C., Lonsdale, P., 1997. Structural variation in the outer rise of the Middle America Trench, (abstract). *EOS* 78, F637.
- McAdoo, B., Orange, D., Silver, E., McIntosh, K., Abbott, L., Galewsky, J., Kahn, L., Protti, M., 1996. Seafloor structural observations, Costa Rica accretionary prism. *Geophys. Res. Lett.* 23, 883–886.
- Menard, H.W., 1978. Fragmentation of the Farallon plate by pivoting subduction. *J. Geol.* 86, 99–101.
- Meschede, M., Barckhausen, U., 2001. The relationship of the Cocos and Carnegie Ridges: age constraints from paleogeographic reconstructions. *Int. J. Earth Sci.* 90, 386–392.
- Meschede, M., Barckhausen, U., Worm, H., 1998. Extinct spreading on the Cocos Ridge. *Terra Nova* 10, 211–216.
- Molnar, P., Sykes, L.R., 1989. Tectonics of the Caribbean and Middle American regions from focal mechanisms and seismicity. *Geol. Soc. Amer. Bull.* 80, 1639–1684.
- Perfit, M.R., Fornari, D.J., Ridley, W.I., Kirk, P.H., Casey, J., Kastens, K.A., Reynolds, J.R., Edwards, M., Desonie, D., Shuster, R., Paradis, S., 1996. Recent volcanism in the Siquieros transform fault: picritic basalts and implications for MORB magma genesis. *Earth Planet. Sci. Lett.* 141, 91–108.
- Protti, M., Guendel, F., McNally, K., 1995. Correlation between the age of the subducting Cocos plate and the geometry of the Wadati–Benioff zone under Nicaragua and Costa Rica. *Geol. Soc. Am. Spec. Paper* 295, 309–326.
- Ross, M.I., Scotese, C.R., 1988. A hierarchical tectonic model of the Gulf of Mexico and Caribbean region. *Tectonophysics* 155, 139–168.
- Sandwell, D., Smith, W., 1997. Marine gravity anomaly from Geosat and ERS1 satellite altimetry. *J. Geophys. Res.* 102, 10039–10054.
- Sandwell, D.T., Winterer, E.L., Mammerickx, J., Duncan, R.A., Lynch, M., Levitt, D., Johnson, C., 1995. Evidence for diffuse extension of the Pacific plate from Pukapuka ridges and cross-grain gravity lineations. *J. Geophys. Res.* 100, 15087–15099.
- Scheirer, D.S., Forsyth, D.W., Cormier, M.C., Macdonald, K.C., 1998. Shipboard geophysical indication of asymmetry and melt production beneath the East Pacific Rise near the MELT experiment. *Science* 280, 1221–1224.
- Searle, R.C., 1983. Multiple, closely spaced transform faults in fast-slipping fracture zones. *Geology* 11, 607–610.
- Searle, R.C., Francheteau, J., Cornaglia, B., 1995. New observations on mid-plate volcanism and the tectonic history of the Pacific plate, Tahiti to Easter microplate. *Earth Planet. Sci. Lett.* 131, 395–421.
- Sempere, T., Herail, G., Oller, J., Bonhomme, M.G., 1990. Late Oligocene–Early Miocene major tectonic crisis and related basins in Bolivia. *Geology* 18, 946–949.
- Sen, G., Hickey-Vargas, R., Waggoner, D.G., Maurrasse, F., 1988. Geochemistry of basalts from the Dumisseau Formation, southern Haiti; implications for the origin of the Caribbean Sea crust. *Earth Planet. Sci. Lett.* 87, 423–437.
- Shiple, T.H., Moore, G.F., 1986. Sediment accretion, subduction and dewatering at the base of the slope off Costa Rica: a seismic reflection view of the decollement. *J. Geophys. Res.* 91, 2019–2028.
- Shiple, T.H., McIntosh, K.D., Silver, E.A., Stoffa, P.L., 1992. Three-dimensional seismic imaging of the Costa Rica accretionary prism: structural diversity in a small volume of the lower slope. *J. Geophys. Res.* 97, 4439–4459.
- Sigurdsson, H., Kelley, S., Leckie, R., Carey, S., Bralower, T., King, J., 2000. History of Circum-Caribbean explosive volcanism: Ar^{40}/Ar^{39} dating of tephra layers. *Proc. ODP Sci. Results* 165, 299–314.
- van Andel, T.H., Heath, E.R., Malfait, B.T., Heinrichs, D.F., Ewing, J.I., 1971. Tectonics of the Panama Basin, eastern equatorial Pacific. *Geol. Soc. Amer. Bull.* 82, 1508–1689.
- Van Andel, T.H., Heath, G.R., et al., 1973. Site 155. Initial Rep. Deep. Sea Drill. Proj. 16, 53–150.
- von Huene, R., Bialas, J., Flueh, E., Cropp, B., Csernok, T., Fabel, E., Hoffman, J., Emeis, K., Holler, P., Jeschke, G., Leandro, C., Perez, I., Chavarria, J., Florez, A., Escobedo, Z., Leon, R., Barrios, O., 1995. Morphotectonics of the Pacific convergent margin of Costa Rica. *Geol. Soc. Am. Spec. Paper* 295, 291–307.
- von Huene, R., Ranero, C.R., Weinrebe, W., Hinz, K., 2000. Quaternary convergent margin tectonics of Costa Rica, segmentation of the Cocos Plate, and Central American volcanism. *Tectonics* 19, 314–334.
- Warsi, W.E., Hilde, T.W.C., Searle, R.C., 1983. Convergence structures of the Peru Trench between 10°S and 14°S. *Tectonophysics* 99, 313–329.
- Werner, R., Hoernle, K., Barckhausen, U., Hauff, F., 2003. Geodynamic evolution of the Galapagos hot spot system (Central East Pacific) over the past 20 m.y.: constraints from morphology, geochemistry, and magnetic anomalies. *Geochem. Geophys. Geosys.* 4, 1108.
- Westbrook, G.K., Hardy, N.C., Heath, R.P., 1995. Structure and tectonics of the Panama–Nazca plate boundary. *Geol. Soc. Am. Spec. Paper* 295, 91–109.
- White, R., McKenzie, D., 1989. Magmatism at rift zones: the generation of volcanic continental margins and flood basalts. *J. Geophys. Res.* 94, 7685–7729.
- Wilson, D.S., 1996. Fastest known spreading on the Miocene Cocos–Pacific plate boundary. *Geophys. Res. Lett.* 23, 3003–3006.
- Wilson, D.S., Hey, R.N., 1995. History of rift propagation and magnetization intensity for the Cocos–Nazca spreading center. *J. Geophys. Res.* 100, 10041–10056.
- Wortel, R., Cloetingh, S., 1981. On the origin of the Cocos–Nazca spreading center. *Geology* 9, 425–430.
- Yeats, R.S., Forbes, W.C., Heath, G.R., Scheidegger, K.F., 1973. Petrology and geochemistry of DSDP Leg 16 basalts, eastern equatorial Pacific. Initial Rep. Deep Sea Drill. Proj. 16, 617–640.